Chapter 13
Emerging Technologies to Increase the Bioavailability of Poorly Water-Soluble Drugs

Leena Kumari Prasad, Justin R. Hughey, James W. McGinity, Dave A. Miller, and Robert O. Williams III

Abstract The need for novel processes and formulation-based techniques to enhance the solubility of poorly water-soluble drugs has increased substantially in recent years. This is primarily due to the limitations of traditional techniques such as physical and chemical stability of the drug substance or the need for toxic solvents that some techniques require. Alternative solubility-enhancement techniques have emerged in recent years to mitigate issues such as these. The purpose of this chapter is to describe emerging technologies for solubility enhancement, allowing the reader to gain an understanding of their utility.

Keywords KinetiSol® Dispersing (KSD) • 3D printing • Electrostatic spinning • Mesoporous materials • Hot-melt extrusion (HME) • Multilayer tablets • Tablet-in-tablet • Ordered mesoporous silica (OMS)

13.1 Introduction

With the advent of high-throughput screening techniques in drug discovery, the number of compounds reaching the formulation development stage has increased drastically (Lipinski et al. 2001; Lipinski 2004). Consequently, this has given rise to

L.K. Prasad (✉) • J.W. McGinity • R.O. Williams III
Division of Pharmaceutics, College of Pharmacy, The University of Texas at Austin, 2409 University Station, A1920, Austin, TX 78712, USA
e-mail: leena.prasad@utexas.edu; mcginity.jw@austin.utexas.edu; bill.williams@austin.utexas.edu

J.R. Hughey
Banner Life Sciences, 4215 Premier Drive, High Point, NC 27265, USA
e-mail: Justin.Hughey@bannerls.com

D.A. Miller
DisperSol Technologies, LLC, 111 W Cooperative Way, Georgetown, TX 78626, USA
e-mail: dave.miller@dispersoltech.com

R.O. Williams III et al. (eds.), *Formulating Poorly Water Soluble Drugs*, AAPS Advances in the Pharmaceutical Sciences Series 22,
DOI 10.1007/978-3-319-42609-9_13

a dramatic increase in the number of compounds that exhibit poor water solubility. These drug substances may also exhibit instabilities or other properties that severely limit standard processing and formulation techniques. The development of new techniques to improve the bioavailability of compounds such as these has become a major point of interest in the pharmaceutical industry. In recent years, a number of novel processing and formulation techniques have emerged that allow for the successful manufacture and delivery of these compounds.

Emerging technologies that utilize specific processes primarily offer novel methods of forming amorphous solid dispersions (ASD) with traditional materials. These technologies offer alternatives to methods such as spray drying and hot-melt extrusion (HME). Specifically, KinetiSol® Dispersing (KSD), 3D printing, and electrostatic spinning are emerging techniques that have recently been developed for the production of ASDs. Emerging formulation techniques include the use of mesoporous materials as carriers for adsorbed drugs and the preparation of co-amorphous mixtures. The following sections discuss the background of each of these techniques, as well as specific examples that exhibit the advantages of each bioavailability enhancement technique.

13.2 Process-Based Techniques

Solid dispersions have received a significant amount of interest in the scientific literature as a method to improve the oral bioavailability of poorly water-soluble compounds (Serajuddin 1999; Leuner and Dressman 2000; Breitenbach 2002; Crowley et al. 2007). These systems, originally described by Sekiguchi and Obi, contain at least one drug substance dispersed within an inert carrier in the solid state (Sekiguchi and Obi 1961; Chiou and Riegelman 1971). ASDs, in which the drug is molecularly dispersed in a single-phase system, may be prepared by methods that can be broadly classified as being solvent- or fusion-based techniques. Traditional high-throughput manufacturing processes such as spray drying and HME have been used with great success for the production of many solid dispersion systems. However, each technique has inherent disadvantages that may prevent the successful processing of some compounds.

While the spray-drying process has the advantage of utilizing traditional manufacturing equipment, it relies on the use of potentially toxic solvents which must ultimately be recovered and properly disposed of. Dispersions prepared by spray drying often require extended drying steps in order to reduce residual solvent levels to those outlined in International Conference on Harmonization guidelines. Furthermore, the spray-drying process can produce dispersions with relatively low bulk densities requiring additional downstream processing such as roller compaction.

The HME process may not be feasible in cases where the drug substance is thermally labile or shear sensitive. One major disadvantage of this technology is that high temperatures and prolonged residence times are normally required to facilitate the transition from the thermodynamically stable crystalline state to the high-energy amorphous state. Many drug substances are known to degrade at elevated temperatures (Murphy and Rabel 2008; Repka et al. 2003, 1999; Follonier

et al. 1994) and degradation due to thermal exposure has been reported for many pharmaceutically relevant polymers (El'Darov et al. 1996; Crowley et al. 2002; Capone et al. 2007). Simply reducing processing temperature to limit degradation may not be feasible due to viscosity and glass-transition temperature limitations. To circumvent this issue, liquid or solid-state plasticizers may be incorporated into dispersions as a processing aid (Repka et al. 1999; Follonier et al. 1994; Zhu et al. 2002, 2006). While incorporation of a plasticizer does allow for processing at decreased temperatures, it may result in a physically unstable system due to reduced glass transition temperature, T_g, and increased molecular mobility (Hancock et al. 1995; Hancock 2002).

Residence times at elevated temperatures in a HME process will vary with processing conditions, but can be expected to fall within the 1–2 min range and in some cases as long as 10 min (Verreck et al. 2006; Kumar et al. 2008). In order to reduce the residence time in a hot-melt extruder, the level of mixing can often be adjusted by the addition or removal of mixing elements. While reducing the number of mixing elements will, in most cases, decrease residence time, specific shear input is reduced and drug substances may not fully transition to the amorphous state.

13.2.1 KinetiSol® Dispersing

Kinetisol® (KSD) is a fusion-based processing technique for the rapid production of polymeric amorphous solid dispersions. In this high-energy mixing process, a shaft with protruding blades rotates at speeds of up to 3500 rpm within a sealed processing chamber containing a drug-polymer blend. A cross-sectional view of the processing chamber is illustrated in Fig. 13.1. Through a combination of kinetic and thermal energy, compositions are processed into a molten mass without the need for external heat input (DiNunzio et al. 2010c). Along with the molten transition, KSD rapidly

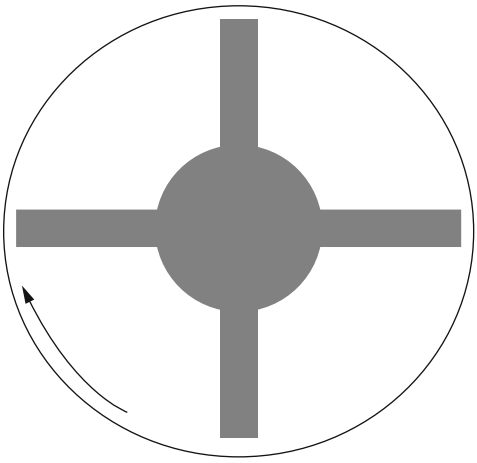

Fig. 13.1 Cross-sectional view of the KinetiSol® Dispersing processing chamber. Reproduced with permission from DiNunzio et al. (2008)

Fig. 13.2 Kinetisol® KC254B Compounder for batch-mode operation (Courtesy of Dispersol Technologies)

and thoroughly mixes the API with the excipient(s) on a molecular level to achieve single-phase, homogenous ASD systems. A computer-control module monitors the real-time temperature of the composition and upon reaching the ejection temperature set point the molten material is ejected. Total processing times are typically less than 20 s and elevated temperatures are generally maintained for less than 5 s, thus significantly reducing the time the drug-polymer system is exposed to elevated temperatures.

KSD compounders can be operated in batch mode or as a semi-continuous process. The batch-mode KSD compounder (Model: KC254B) is shown in Fig. 13.2 and the semi-continuous compounder (Model: KC254C) is shown in Fig. 13.3; the semi-continuous unit enables automated feeding and quenching operations every 0.5–2 min with product throughput of 20–30 kg/h. The proof of concept work with KSD for pharmaceutical ASD systems was first evaluated on industrial-scale compounders with batch sizes from 1 to 10 kg (Miller 2007); however, it has since been scaled down to accommodate pharmaceutical development with further reduced material needs.

DiNunzio et al. conducted early evaluations of the KSD technology to prepare solid dispersions of itraconazole (ITZ) (DiNunzio et al. 2010c, d, b, 2008). Compositions of ITZ with hypromellose (hydroxypropyl methyl cellulose, HPMC) and Eudragit® L100-55 prepared using KSD showed comparable or more rapid drug release in-vitro those prepared by HME; this finding did not show a significant difference in-vivo using a rat model (DiNunzio et al. 2008, 2010c). However, KSD was shown to prepare dispersions that were more homogenous, as seen by single T_g values with thermal analysis, and more physically stable, as they did not require a

Fig. 13.3 Kinetisol® KC254C Compounder for semi-continuous operation (Courtesy of Dispersol Technologies)

plasticizer for processing, as is often the case with HME (DiNunzio et al. 2010b, c). The authors showed that 1:2 compositions of ITZ:Eudragit® L100-55, an enteric polymer with concentration enhancing properties, could not be effectively processed by HME due to high viscosity and decomposition of the polymer (DiNunzio et al. 2010b). Triethyl citrate (TEC) was incorporated into HME compositions at 20 % (by dry polymer weight) as a processing aid. Conversely, compositions containing a 1:2 ratio of ITZ: Eudragit® L100-55 were successfully processed by KSD, primarily due to the high torque output inherent to this technology. All samples were determined to be amorphous by powder x-ray diffraction (PXRD). Furthermore, modulated DSC analysis showed that the HME and KSD compositions exhibited glass transition temperatures of 54.2 °C and 101.3 °C, respectively; the lower T_g of the HME due to the incorporation of TEC. Milled samples were placed at accelerated stability conditions (40 °C/75 % RH) for 6 months to evaluate the physical stability of compositions prepared by each processing method. As shown in Fig. 13.4, crystalline peaks identified as those characteristic of ITZ were found in HME compositions at the 3- and 6-month time points, indicating physical instability due to increased molecular mobility. Compositions prepared by KSD exhibited physical stability over the same 6-month testing period. Since these studies, the application of KSD has evolved to increase the formulation design space for amorphous solid dispersions, including the ability to process high melting point and thermally sensitive materials and high viscosity polymer carriers, which are particularly difficult to process using HME and spray-drying processes.

With HME processing, temperatures must be sufficiently high to produce molten material to enable proper mixing and dispersion and/or solubilization of the drug into the polymer carrier; this is usually 15–30 °C above the melting point of the drug substance and/or polymer. Thus, with high melting point drugs, high processing temperatures would be required, which could be detrimental to the chemical stability of

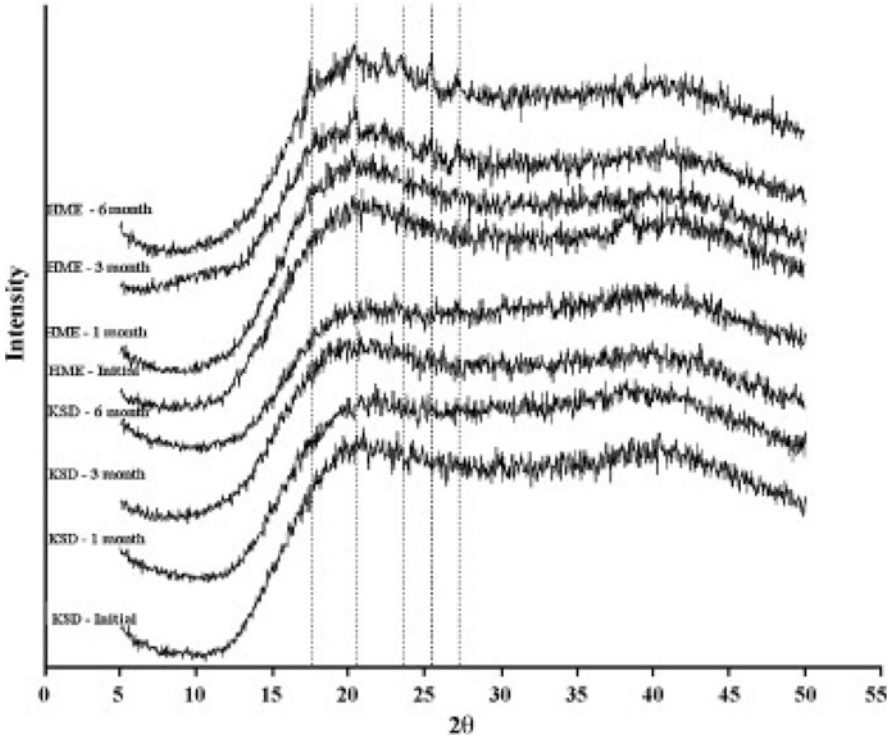

Fig. 13.4 PXRD patterns of HME and KSC ITZ:Eudragit L100-55 solid dispersions measured over 6 months accelerated stability at 40 °C/75 % RH. Samples were stored in 30 cc HDPE induction sealed bottles. Reproduced with permission from DiNunzio et al. (2010b)

the drug and/or polymer (Lakshman et al. 2008; LaFountaine et al. 2015b). Alternatively, a substantial amount of plasticizer would be required to reduce processing temperatures, which could reduce the physical stability of the solid dispersion (Verreck 2012). The high shear rates imparted by the KSD accelerate the solubilization kinetics of a compound in a molten polymer, which allows processing temperatures below the melting point of the drug. Because of this, the production of ASD systems with high melting point materials (T_m > 225 °C) is possible with KSD processing. Hughey et al. demonstrated the ability to process high melting point drugs with the KSD process, using meloxicam (MLX) with a melting point of 270 °C as a model compound (Hughey et al. 2011). This study utilized Soluplus® as the polymer carrier. KSD, at all rotor speeds and ejection temperatures studied, rendered all samples amorphous; however, higher ejection temperatures yielded more MLX degradation. With 3000 rpm rotor speed and an ejection temperature of 110 °C, 98.6 % MLX recovery was obtained from the final dispersion. Extrusion was carried out at temperatures up to 175 °C; however, dispersions still exhibited a low degree of residual crystallinity when the molten material was recirculated for 2 min. Additionally, the longer residence time led to degradation, with only 87.1 % MLX recovery.

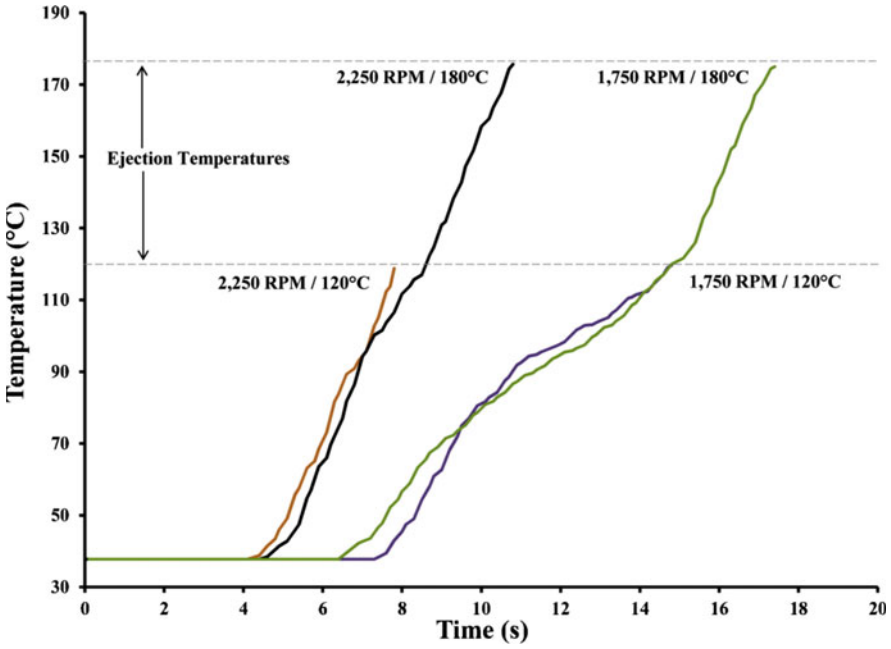

Fig. 13.5 KSD temperature profiles for 1:2 ITZ:HMPC E50LV compositions. Reproduced with permission from Hughey et al. (2012)

More recently, KSD was utilized to prepare amorphous solid dispersions of acetyl-11-keto-b-boswellic acid (AKBA) with a melting point of 295 °C, a compound unable to be extruded due to its high melting point and thermal liability (Bennett et al. 2013). KSD was able to render AKBA amorphous with four different polymeric carriers: HPMCAS-LF, HPMCAS-MF, Eudragit® L100-55, and Soluplus® in combination with Eudragit® L100-55 with potency of greater than 99 %.

In addition to being able to process high melting point drug substances, the short processing times and lower ejection temperatures with KSD were shown to allow processing of thermally labile drugs (DiNunzio et al. 2010a; Hughey et al. 2010). The short residence times of the KSD process can also benefit the thermal stability of the polymer carrier; additionally, the high torque outputs allow for the ability to process high viscosity, high molecular weight carriers—both of these increasing the options for polymeric carriers of amorphous solid dispersion systems. Hughey et al. showed that the within a given chemistry of cellulosic polymers, the higher the degree of ITZ supersaturation was seen with increasing viscosity, albeit up to a point (Hughey et al. 2012). HPMC E50LV was evaluated as one of the promising viscous polymers for ITZ supersaturation; however, at HME processing temperatures above its T_g, HPMC has been shown to brown/darken and chemically degrade (LaFountaine et al. 2015b; Coppens et al. 2004). Hughey et al. evaluated the effect of processing conditions, shown in Fig. 13.5, and found that the polymer degradation was related to both shear and thermal energy input, as well as the interaction

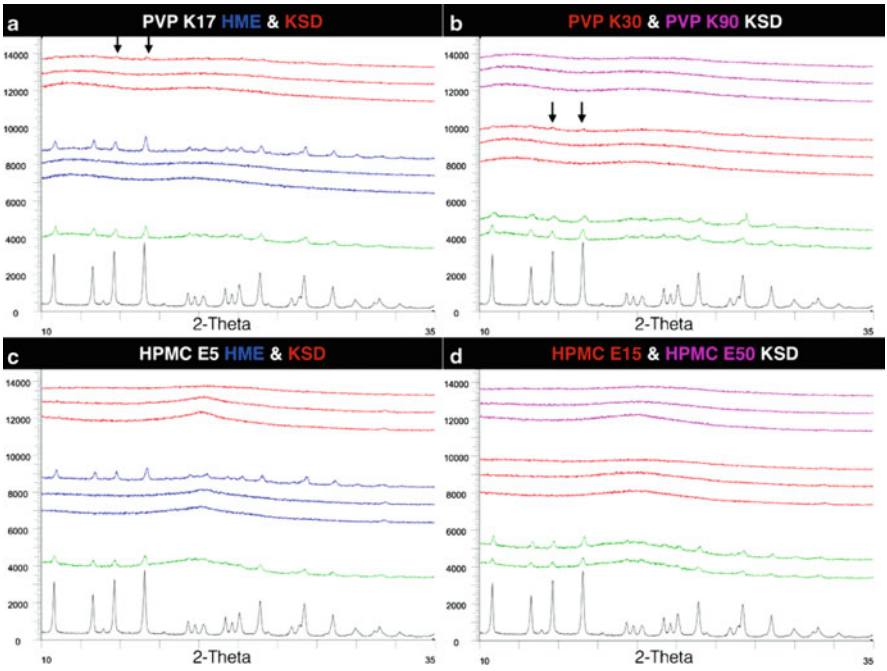

Fig. 13.6 PXRD profiles (from *bottom to top*) of GRIS crystalline drug (▬ ▬), 10 % drug load physical mixtures (▬ ▬), HME processed dispersions (▬ ▬), and KSD processed dispersions (▬ ▬) (from 10 to 40 % drug load) in (**a**) (PVP K17) and (**c**) (HPMC E5). KSD processed dispersions of PVP K30 (▬ ▬) and PVP K90 (▬ ▬) (from 10 to 40 % drug load) in (**b**) and KSD processed dispersions of HPMC E15 (▬ ▬) and HMPC E50 (▬ ▬) (from 10 to 40 % drug load) in (**d**). Reproduced with permission from LaFountaine et al. (2015a)

between the two suggesting the polymer chains may be more susceptible to shearing forces at higher temperatures. KSD was able to render the ITZ: HPMC E50LV compositions amorphous, including with increasing drug load up to 50 % w/w, with limited polymer degradation and no noticeable browning at processing speeds of 2250 rpm and ejection temperature of 120 °C, significantly lower than the melting point of both the drug or polymer.

LaFountaine et al. systematically investigated the processability of increasing polymer molecular weight and thus viscosity using HPMC (E5, E15, and E50) and polyvinylpyrrolidone (PVP) (K17, K30, and K90) using HME and KSD with griseofulvin (GRIS) as a model drug (LaFountaine et al. 2015a). As seen with previous studies, HPMC E15, HPMC E50, PVP K30, and K90 were not amenable to HME processing without a plasticizer (Fousteris et al. 2013; Ghebremeskel et al. 2006). Additionally, the HME dispersions prepared with HPMC E5 and PVP K17 were phase separated at higher drug loads, as shown in Fig. 13.6. However, KSD was able to prepare amorphous dispersions for all polymer grades at drugs loads of 10, 20 and 40 %, with the exception of a small degree of residual crystallinity seen in

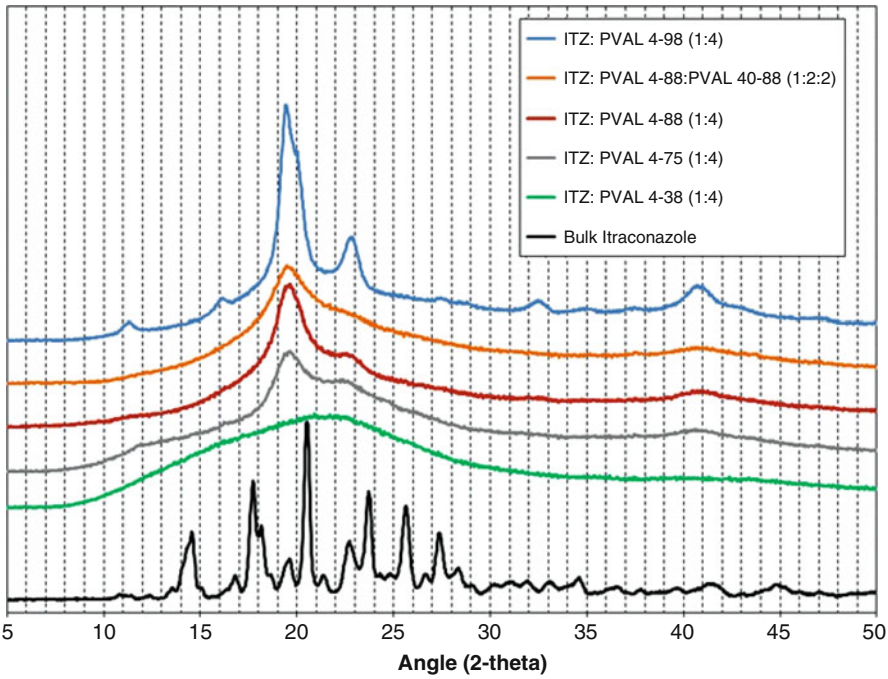

Fig. 13.7 PXRD profiles of (from *bottom* to *top*) bulk ITZ, ITZ: PVA 4-38 (1:4), ITZ: PVA 4-75 (1:4), ITZ: PVA 4-88 (1:4), ITZ: PVA 4-88: 40-88 (1:2:2) and ITZ 4-98 (1:4). Reproduced with permission from Brough et al. (2015)

the PVP K30 40 % drug load formulation. Although, GRIS, a proton acceptor, is expected to interact with PVP, a proton acceptor, no chemical interaction was seen via FTIR or FT-Raman analysis. After 6 months at open dish accelerated stability conditions (40 °C/75 % RH), all formulations showed no physical change via PXRD. With no chemical interactions, the stabilization of these systems was attributed solely to decreased molecular mobility.

The ability of KSD to process materials not previously amenable to thermal processing or spray drying due to melting point and viscosity limitations has opened the door to evaluating polymers that were thus far not considered for ASDs. Polyvinyl alcohol (PVA) is a hydrophilic, non-toxic, semi-crystalline polymer often utilized as a stabilizing agent in emulsions, a viscosity increasing agent or lubricant in ophthalmic and topical solutions, as well as in composite biodegradable materials (Rowe et al. 2012). The high viscosity and melting point of the polymer limits its use in HME as it requires up to 40 % plasticizer to reduce processing temperatures, particularly with PVA grades with a high degree of hydrolysis (De Jaeghere et al. 2015). Brough et al. evaluated PVA grades with varying degrees of hydrolysis with ITZ, showing that KSD processing was able to render the ITZ amorphous, while the PVA retained its crystalline structure (Brough et al. 2015), as shown in Fig. 13.7. The PVA 4-88 and 4-75 grades, indicative of 88 and 75 % hydrolysis, respectfully

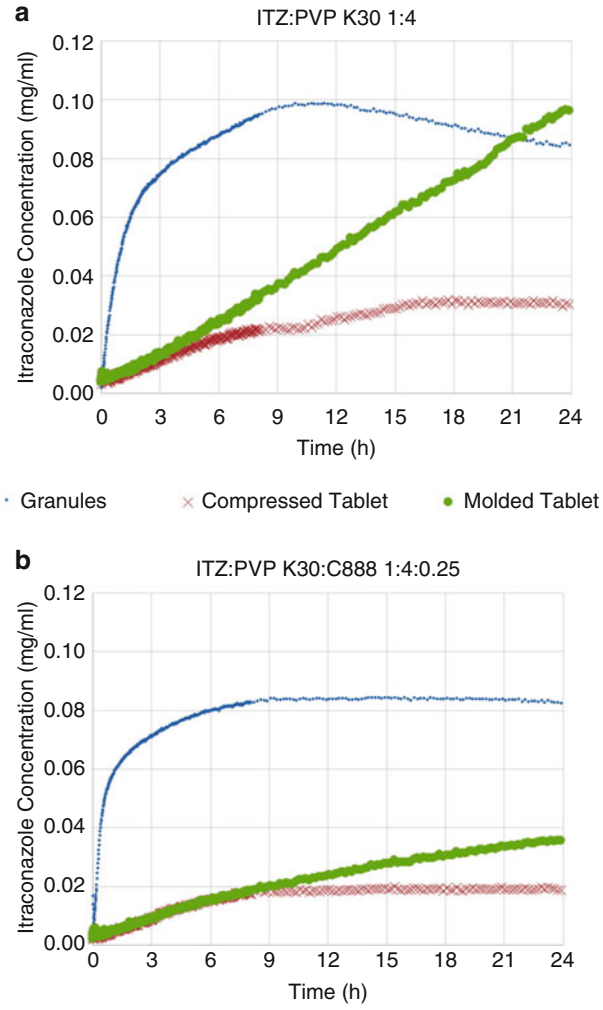

Fig. 13.8 ITZ dissolution rates measured by USP Method II at 50 rpm at 37 °C in 0.1 N HCl: (**a**) ITZ and PVP solid dispersions at 0.2 mg/mL at ITZ concentration; (**b**) ITZ, PVP, and C888 solid dispersions at 0.2 mg/mL ITZ concentration. Reproduced with permission from Keen et al. (2015)

(Note: 98 % is considered fully hydrolyzed), showed rapid and full drug release, as the highly hydrolyzed grades are more water-soluble.

With the ability to prepare higher drug loads, KSD offers a significant advantage to reduce pill size and pill burden. Hughey et al. investigated a 1:3 carbamazepine (CBZ): Soluplus® formulation at a 70 % dispersion loading in tablet and found that the drug release was slowed after compression, with less than 80 % release in 2 h compared to the 100 % drug release in less than 30 min from the dispersion alone in 0.1 N HCl dissolution media (Hughey et al. 2013). The addition of potassium bicarbonate at levels as low as 1 % to the tablet formulation allowed for rapid disintegration to obtain a release profile similar to that of the dispersion alone. In another study,

Hughey et al. incorporated a low-substituted grade of hydroxypropyl cellulose (HPC), a compressible superdisintegrant, in the dispersion composition for nifedipine (NIF): HPMCAS to improve disintegration properties after tablet compression, finding that the intragranular disintegrant enabled higher drug release in the acid phase due to improved wetting (Hughey et al. 2014). Alternatively, Keen et al. evaluated the use of KSD to prepare monolithic tablets direct shaping/molding from the ejected KSD molten mass (Keen et al. 2015). To prepare a controlled release tablet formulation of ITZ, high molecular weight PVP K30 was utilized as the polymer carrier and glyceryl behenate (Compritol 888 ATO, C888), a hydrophobic lipid, as the release modifier and plasticizer. When compared to ITZ: PVP K30 formulations with and without C888 prepared by HME, followed by milling and tablet compression, the monolithic tablet exhibited a zero order release with a slowed release from the C888 containing formulations, while the compressed tablets showed a plateau in drug release as shown in Fig. 13.8, attributed to water ingress into tablet pores that enabled local precipitation.

13.2.2 3D Printing

The FDA approval of the first 3D printed tablet, Spritam®, set a precedence for the use of 3D printing for the manufacture of dosage forms. Printing boasts capabilities for dispensing low volumes with accuracy, spatial control, and layer-by-layer assembly to prepare complex compositions and geometries. 3D printing is defined as a form of additive manufacturing whereby a structure is assembled by depositing or binding materials in successive layers to produce a 3D object (Chua et al. 2014). Previously utilized as a subset of rapid prototyping to quickly fabricate models and prototypes, 3D printing it is now being developed a scalable manufacturing process and has become more prevalent in biomedical and drug delivery applications over the last 30 years (Günther et al. 2014; Dimov 2001; Rowe et al. 2000; Alomari et al. 2015; Goyanes et al. 2015a; Daly et al. 2015; Goyanes et al. 2015b; Skowyra et al. 2015; Iulia et al. 2003; Boehm et al. 2011). On-going development activities have opened the path to utilizing printing techniques for poorly soluble compounds, particularly with fused deposition modeling (FDM) which utilizes some common thermoplastic polymer carriers as the feed material.

13.2.2.1 Fused Deposition Modeling

Fused deposition modeling (FDM), also referred to as fused filament modeling (FFM), is conducted by feeding thermoplastic filament(s) via roller; the filament is heated by heating elements/liquefier into a molten state to allow for extrusion through the nozzle tip. Upon deposition, the material cools or is cooled and solidifies and the final structure is built in a layer-by-layer fashion, as shown in Fig. 13.9. Some polymers, such as polylactic acid (PLA), PVA, and acrylonitrile butadiene

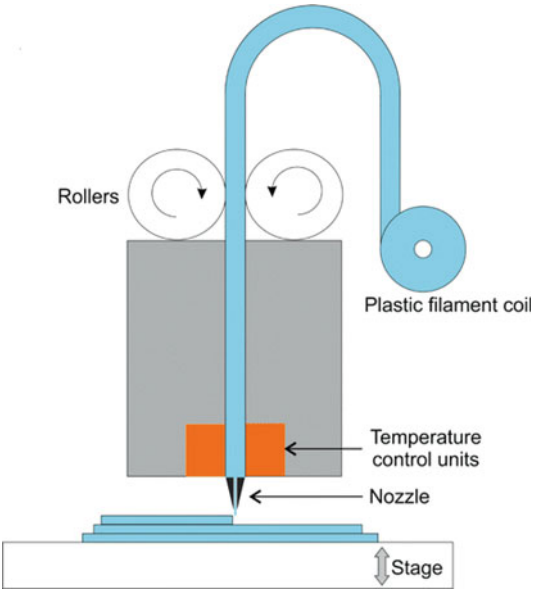

Fig. 13.9 Schematic of fused deposition modeling (FDM) printer. Reproduced with permission from Gross et al. (2014)

styrene (ABS), are commonly used with the FDM process and are commercially available as pre-processed filaments. More recently, FDM has expanded to include the deposition of any material that can flow through a nozzle or syringe and harden or be hardened for layer-by-layer assembly of a structure/dosage form (Campbell et al. 2012; Malone and Lipson 2007).

Skowyra et al. incubated commercially available PVA filaments in a methanol solution of prednisolone (PDN) for 24 h (Skowyra et al. 2015). The methanol was chosen to both solubilize the poorly water soluble PDN and reduce swelling of the PVA filament. After drying, a drug load of approximately 1.9 % was achieved, with the adsorbed PDN mostly in the amorphous state from the evaporation of the methanol. The drug-loaded filament was then used with a FDM printer to prepare tablets with varying size and, thus, varying doses, 2–10 mg. With a low drug loading and residual crystallinity, most probably due to the rate of drying, incubation may not be optimal for the preparation of amorphous solid dispersion filaments for use with FDM. However, filaments can be prepared by HME or by an extruder incorporated upstream from the printer nozzle to allow for more flexibility on composition, including the incorporation of an active drug substance for the preparation of an ASD as the feed filament (Hoque et al. 2012; Sandler et al. 2014; Wang et al. 2004; Hamid et al. 2011).

Goyanes et al. prepared drug loaded PVA filaments with each APAP and caffeine (CAF) using HME to prepare filaments for use with FDM (Goyanes et al. 2015b). Fixed dose combination (FDC) tablets were prepared with multilayered and tablet-in-tablet geometries containing both drugs, as shown in Fig. 13.10. APAP was rendered amorphous during the HME process, but the CAF remained dispersed in its crystalline

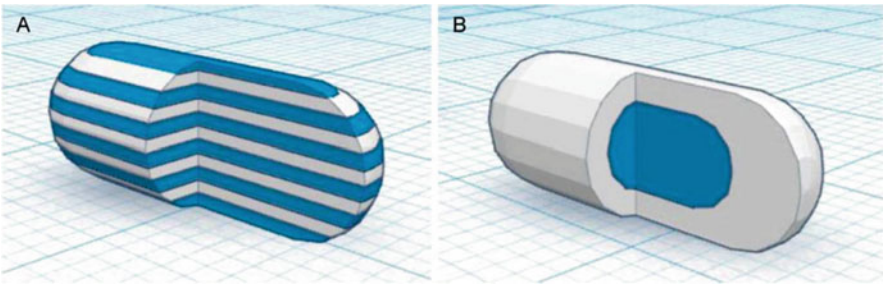

Fig. 13.10 Schematic of (**a**) multilayer and (**b**) tablet-in-tablet geometry for acetaminophen and caffeine FDC tablets. Reproduced with permission from Goyanes et al. (2015b)

state. The multilayered tablets exhibited synchronous release of both drugs, while the tablet-in-tablet geometry showed delayed release of up to 135 min of the inner component when the outer layer was APAP and up to 90 min delayed release when the outer layer was CAF, shown in Fig. 13.11. Longer delayed release was observed when the drug loading was lower, as the PVA levels are higher and control the erosion-based drug release. This study showed the ability to make complex geometries to control drug release using HME to prepare ASD as feed filament.

13.2.3 Electrostatic Spinning

Electrostatic spinning is a technique that has been used successfully in the polymer industry for many years to produce a variety of products, such as separation membranes (Doshi and Reneker 1993; Reneker and Chun 1996). As applied in the polymer industry, a polymer in solution is drawn through a capillary tube that is subjected to an electric field. As the electric field intensity is increased, the solution forms a Taylor cone at the tip of the capillary tube. Once the electric field overcomes the force of surface tension, the solution is ejected in the form of an electrically charged jet. As the solvent evaporates, narrow unwoven filaments are formed that have diameters ranging from 50 nm to 5 μm (Doshi and Reneker 1993). An illustration of a simple electrostatic spinning process is shown in Fig. 13.12. Factors affecting the overall diameter of the electrostatically spun fibers include, but are not limited to, polymer solution viscosity, surface tension of the polymer solution, electric field strength, feed rate, and dielectric constant (Deitzel et al. 2001). This technique was then applied to the pharmaceutical industry for both controlled and immediate release applications (Baldoni and Ignatious 2001; Igantious and Sun 2004; Kenawy et al. 2002; Verreck et al. 2003a, b). In pharmaceutical applications, a drug substance and polymer are dissolved in a solvent system, as would be required in a spray-drying process. In another embodiment, the polymer could be melted in a solvent-free system, provided that the drug substance and polymer are not thermally labile and the resulting viscosity

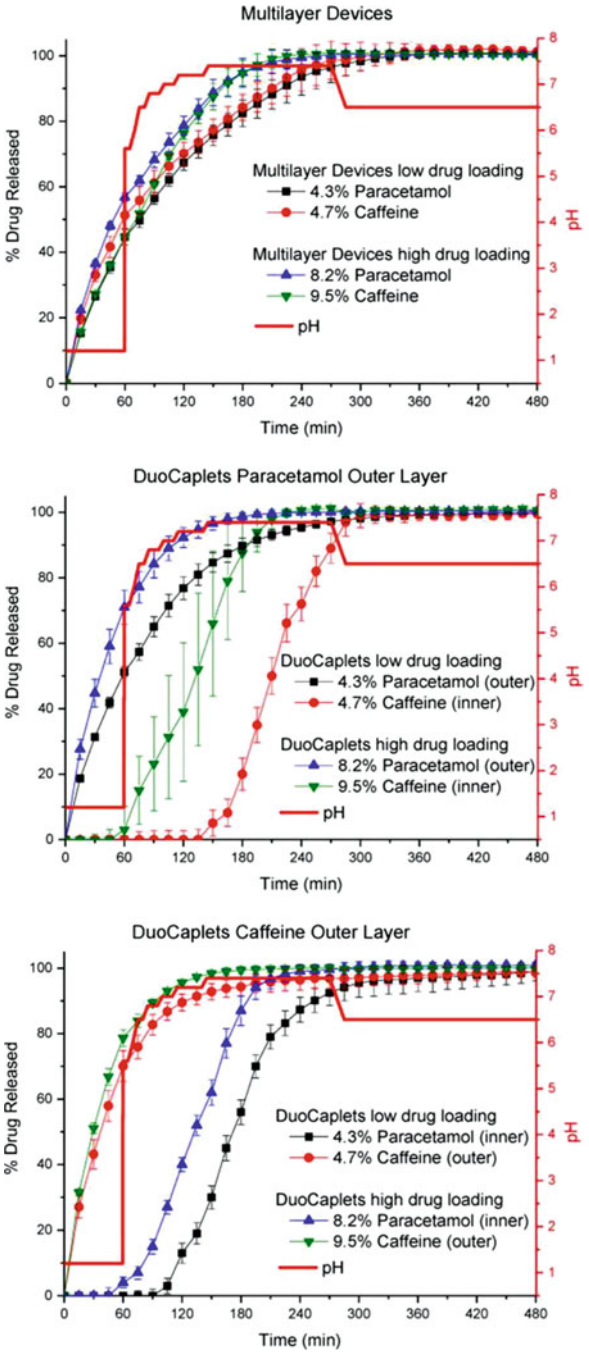

Fig. 13.11 Drug release from multilayered tablets (*top*) and tablet-in-tablet (DuoCaplet) with APAP outer layer (*middle*) and CAF outer layer (*bottom*) prepared with varying drug load. Reproduced with permission from Goyanes et al. (2015b)

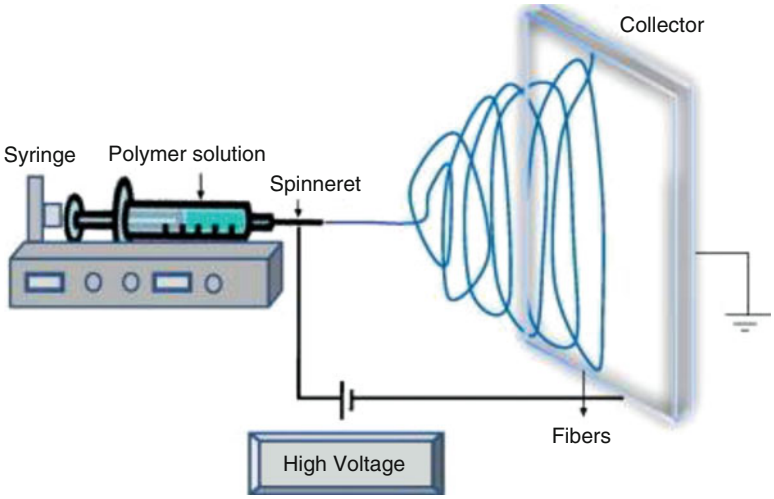

Fig. 13.12 Schematic of electrostatic spinning system in a (**a**) vertical set-up and (**b**) horizontal set-up. Reproduced with permission from Bhardwaj and Kundu (2010)

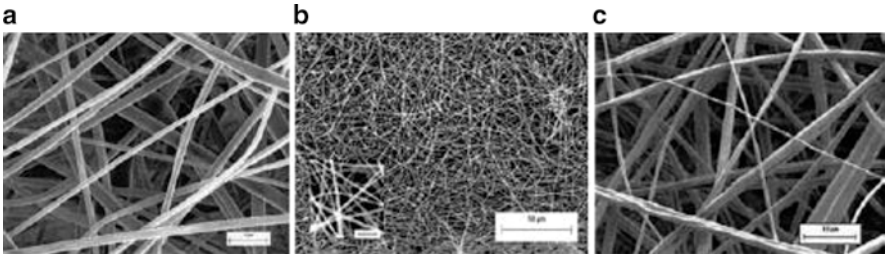

Fig. 13.13 Scanning electron micrograph of (**a**) ITZ/HPMC 40:60 w/w electrostatically spun fibers at 16 kV (magnification 2000×), (**b**) ITZ/HPMC 40:60 w/w electrostatically spun fibers at 24 kV (magnification 500×). In the insert (magnification 8500×), the bar represents 3 μm, and (**c**) ITZ/HPMC 20:80 w/w electrostatically spun fibers at 24 kV (magnification 2000×). Reproduced with permission from Verreck et al. (2003a)

is sufficiently low; this process is also referred to as melt electrospinning (MES) (Ignatious et al. 2010).

In one of the first pharmaceutical-related studies, Verreck et al. investigated the use of electrostatic spinning for the preparation of hydrophilic amorphous solid solutions containing ITZ (Verreck et al. 2003a). HPMC-based compositions containing 20 % (w/w) and 40 % (w/w) ITZ were prepared in an ethanol and methyl chloride co-solvent system. A solids concentration of 12 % (w/w) was chosen based on optimal viscosity. A voltage of 16 or 24 kV was applied and unwoven fibers were collected. Fibers containing 40 % ITZ processed at 16 and 24 kV were found to have diameters ranging from 1 to 4 μm and 300–500 nm, respectively, as

shown in Fig. 13.13a, b. However, as the drug loading was decreased to 20 % and processed at 24 kV, fiber diameters ranged from 500 nm to 3 μm, as shown in Fig. 13.13c. These findings demonstrated that drug concentration within the fiber and the electric potential applied can both have a significant impact on the morphology of the resulting fiber.

Unmilled fibers were found to be amorphous in nature and showed no signs of crystalline character, but the presence of a solid solution was not verified. It was found that when milled, the composition containing 40 % ITZ exhibited a small degree of crystallinity. An in vitro dissolution analysis of the unmilled fibers in 0.1 N HCl showed complete ITZ release; however, the rate was slower than that of solvent cast films and HME-processed compositions.

Ignatious et al. further demonstrated the utility of electrostatic spinning for the preparation of solid dispersions (Ignatious et al. 2010). In this work, the researchers evaluated three compounds in poly(ethylene oxide) (POLYOX®), polyvinylpyrrolidone-vinyl acetate copolymer (PVPVA), and poly(vinyl pyrrolidone) (PVP) matrices. In one example by Ignatious et al., a proprietary compound (Compound I) was electrostatically spun in a PVP matrix at a concentration of 40 % and demonstrated by DSC and XRPD analyses to be amorphous. The nanofibers were dosed to fasted adult male beagle dogs to assess their absorption. Similarly, compressed nanofibers (pellets), non-milled compound I, and wet-bead-milled compound I were assessed. The plasma AUC values demonstrated that wet-bead-milled compound I provided the highest degree of absorption, followed by the nanofibers, nanofiber pellets, and non-milled compound I. The researchers stated that the nanofiber composition could be optimized to further improve absorption.

In a second example by Ignatious et al., another proprietary compound (compound II) was formulated by electrostatic spinning in both POLYOX® and Eudragit® L100-55 matrices. The in vitro dissolution rates were studied at pH values of 1.0 and 7.5, as illustrated in Fig. 13.14. At pH 1.0, the matrix utilizing POLYOX® exhibited release rates similar to a nano-milled formulation. The dissolution rate of Eudragit® L100-55-based matrices was very low due to its poor solubility at this pH value. At a dissolution medium pH of 7.5, the Eudragit® L100-55-based electrostatically spun formulation provided a significantly faster dissolution rate than the nano-milled formulation and the POLYOX®-based fibers. This dissolution rate increase was primarily due to the amorphous nature of compound II and/or the concentration enhancing properties of Eudragit® L100-55.

More recently, coaxial electrospinning was utilized to prepare a multi-component fiber system (Yu et al. 2011). For this system, a core formulation was prepared using acyclovir and PVP, with a surrounding sheath consisting of PVP, sodium dodecyl sulfate, and sucralose. With a high melting point (257 °C) and poor solubility in water, as well as many organic solvents, acyclovir was especially challenging to process using conventional HME or spray drying methods. However, using coaxial electrospinning, the core solution of 10 %w/v PVP and 2 %w/v acyclovir in a dimethylacetamide: ethanol (4:6), not typically amenable to electrospinning, was able to be processed as the sheath solution, consisting of 10 %w/v PVP, 0.5 %w/v SDS, and

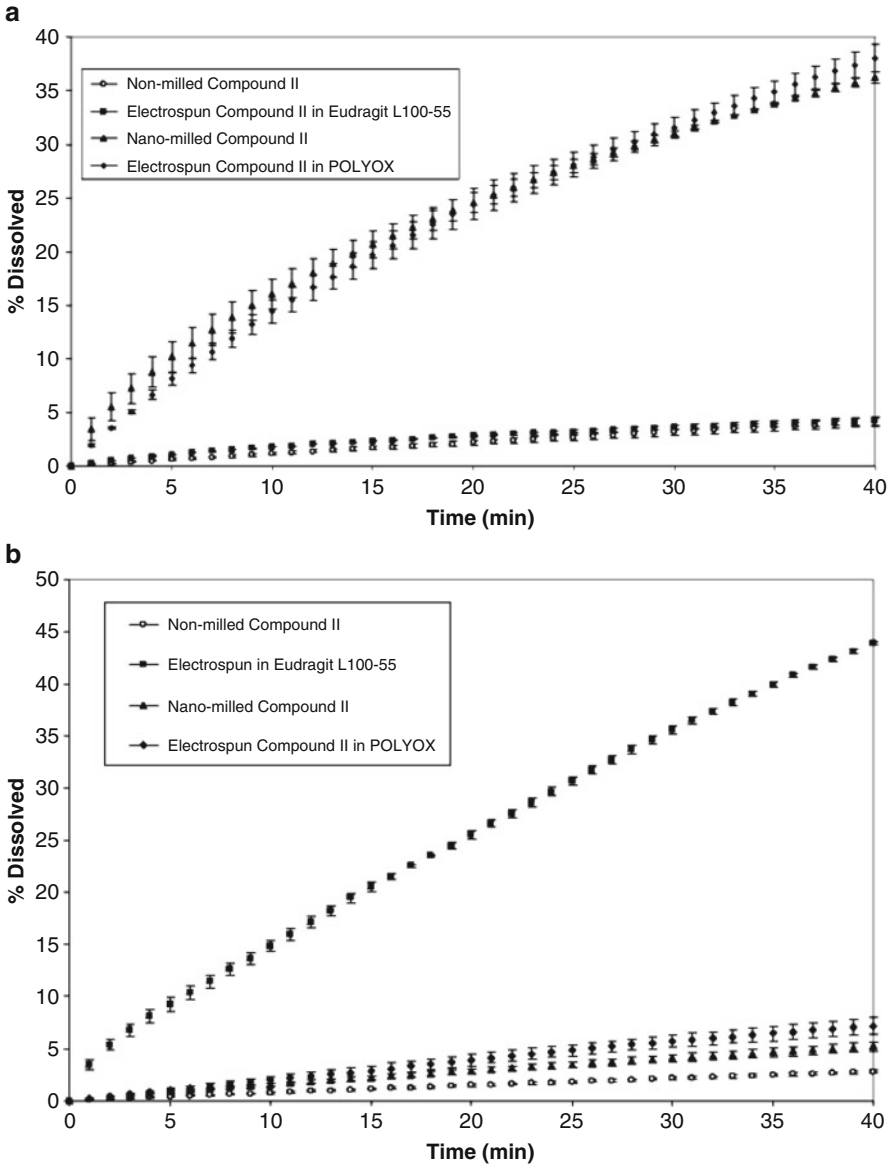

Fig. 13.14 In vitro dissolution profiles of Compound II at (**a**) pH 1.0 and (**b**) pH 7.5. Reproduced with permission from Ignatious et al. (2010)

0.2 %w/v sucralose in a water:ethanol (2:8) acted as a guide, enabling the formation of core-sheath nanofibers. These prepared fibers resulted in rapid drug release, 100 % within 1 min due the amorphous nature of the drug and high surface area, compared to the 40 % drug release in 60 min from micronized (<100 μm) acyclovir particles.

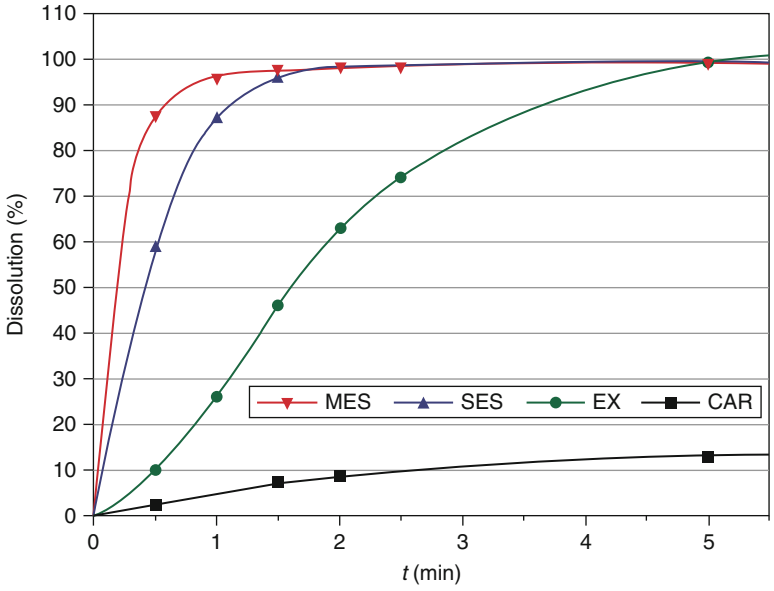

Fig. 13.15 CAR drug release in 900 mL 0.1 M HCl, USP II at 50 rpm. (*MES* melt electrospun fibers, *SES* solvent-based electrospun fibers, *EX* HME particles, *CAR* unprocessed crystalline carvedilol). Reproduced with permission from Nagy et al. (2013)

Nagy et al. conducted a study to evaluate the properties of a dispersion of carvedilol (CAR) with Eudragit® E prepared using HME, electrospinning, and MES (Nagy et al. 2013). All methods produced amorphous solid dispersions with a 20 % drug load; however, the mean fiber diameter of the MES material was significantly larger than that from electrospinning, 250 μm versus 0.7 μm, respectively, which also resulted in lower specific surface area with the MES fibers. The HME particles were milled to 20 μm mean particle size, and they were all evaluated for drug release against he crystalline CAR, as shown in Fig. 13.15. Surprisingly, the MES material, with larger fiber diameter and lower surface area, exhibited a faster release profile than the electrospun fibers; while both fibers showed faster release than the HME particles. A similar drug release trend was seen with CAR from a copovidone (PVPVA 64) carrier (Balogh et al. 2015). As with HME, plasticizers can be added to reduce processing temperatures as needed (Balogh et al. 2014).

Electrostatic and MES are promising processes to produce ASDs that exhibit very large surface areas due to the production of nano- and micro-sized fibers. The rapid drying of the solvent-based electrospinning process is able to produce amorphous drug molecules dispersed in the polymer matrix and allow for higher drug loading than HME (Nagy et al. 2012; Yu et al. 2011). The continued development of the electrospinning process has allowed for the introduction of new techniques,

such as coaxial electrospinning, for pharmaceutical dosage form design and will continue to lead to more novel and multi-functional dosage forms.

13.3 Formulation-Based Techniques

While the formation of ASDs is an effective technique to enhance the bioavailability of poorly water-soluble compounds, there are a variety of other formulation-based techniques that can achieve the same goal. Many of these techniques are covered in previous chapters, including formation of salts, co-crystals, co-solvent or complexed systems, and lipid based or self-emulsifying drug delivery systems. However, some of these systems have limitations, such as toxicity limits with surfactants and other lipids; thus, formulation techniques continue to be developed for bioavailability enhancement.

13.3.1 Mesoporous Materials

Mesoporous materials, defined as having pore diameters from 2 to 50 nm, have emerged as promising carriers for poorly soluble compounds. The distribution of nanosized pores provides a high surface area for drug loading and thin channels that prevent formation of highly ordered crystals, maintaining deposited drug in its metastable amorphous state (Wang et al. 2010). Additionally, the pore size or surface chemistry of the material can be readily tailored to allow for immediate, sustained or controlled release of the adsorbed drug (Wang et al. 2015).

13.3.1.1 Mesoporous Silica

Ordered mesoporous silica (OMS) materials were discovered in the early 1990s by the Mobil Corporation for use in a broad range of applications such as catalysis and optics; however, by 2001, these high surface area and highly porous materials were being evaluated as carriers for drug delivery (Vallet-Regi et al. 2001). With the recent clinical approval of the Cornell Dots (C dots), the safety of these inorganic materials is being evaluated, opening the door for future clinical studies for OMS for drug delivery (Bradbury et al. 2015).

OMS materials can have a wide range of mesostructures from 1D lamellar to tetragonal (Garcia-Bennett et al. 2005); however, the most commonly used OMS materials for drug delivery are characterized as having a 2D hexagonal or 3D cubic mesostructures, as shown in Fig. 13.16. Materials are available in a wide range of mesopore diameters (2 nm $< Dp <$ 50 nm) and have relatively large pore volumes of 0.6–1.0 mL/g (Mamaeva et al. 2013). Two of the most commonly used OMS mate-

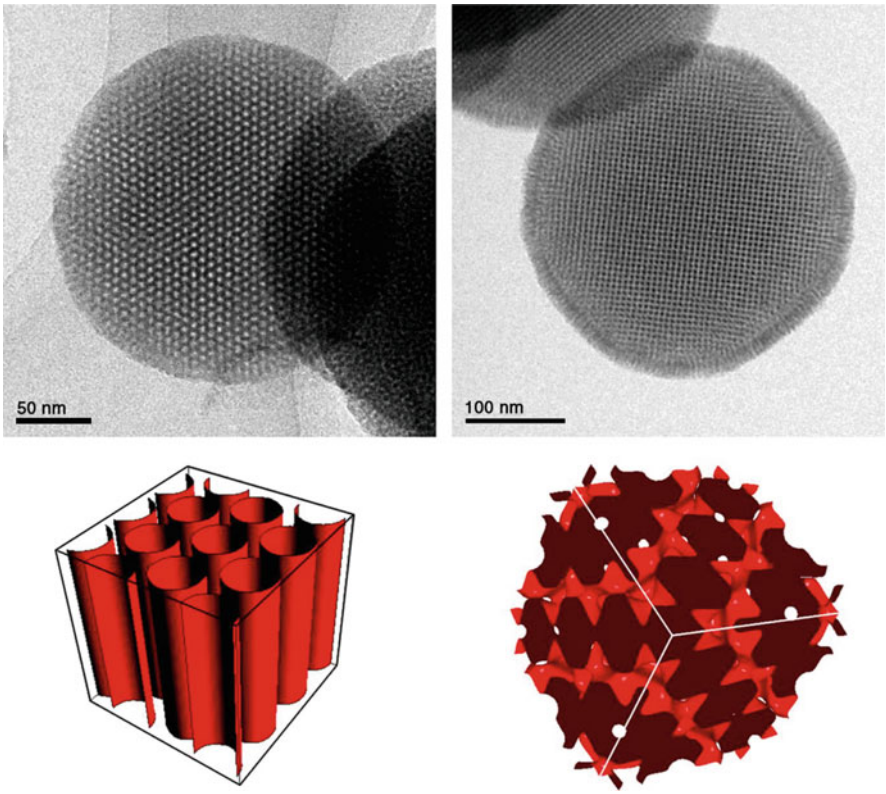

Fig. 13.16 TEM image (*left top*) and model of unit cell (*left bottom*) of 2D hexagonal mesostructure and TEM image (*right top*) and model unit cell (*right bottom*) of 3D cubic mesostructure. Reproduced with permission from Fadeel and Garcia-Bennett (2010)

rials investigated in recent years are MCM-41 (Mobil Composition of Matter No. 41) and SBA-15 (Santa Barbara Amorphous No. 15) (Mellaerts et al. 2008b; Wang et al. 2013). The pore diameter ranges between 2 and 10 nm for MCM-41 and 5 and 15 nm for SBA-15 (Zhao et al. 1998). Note that SBA-15 can be prepared to exhibit a 2D hexagonal or 3D cubic structure (Kruk et al. 2000). In addition to small pore diameters and high pore volumes, these materials have a high surface area (600–1000 m^2/g) and a dense distribution of silanol groups (2–3 groups/nm) to serve as adsorption sites or as sites for complexation with other functional groups, such as carboxylic acids or amines (Mamaeva et al. 2013; Wang et al. 2015).

OMS materials are prepared by a sol–gel or ion reaction method in acid or alkaline conditions to produce homogeneous size particles with the addition of a surfactant as a structure or pore-forming agent. A washing or calcination step is used to remove the surfactant leaving behind empty pores (Kresge et al. 1992; Inagaki et al. 1993). The particle size, pore size and volume, and mesostructures can be readily tailored by processing parameters, such as surfactant type and temperature (Hu et al.

2011). Drug loading and addition of functional groups typically occur post-synthesis. Methods for drug loading include adsorption from solution, electrostatic adsorption, incipient wetness impregnation, the melt method, or co-spray-drying (Mellaerts et al. 2008a; Shen et al. 2010). Adsorption from solution is the most common method for poorly soluble compounds, whereby the OMS particles are immersed in a concentrated organic solution of the active compound and the resulting suspension is dried to remove residual solvent, leaving behind the adsorbed drug. Notably, the polarity of the solvent can affect drug-loading efficiency, as polar solvents will compete for the adsorption sites (Xu et al. 2013).

Vallet-Regi, et al. (2001) first evaluated OMS as a reservoir for controlled drug-delivery systems (Vallet-Regi et al. 2001). In this initial study, the researchers utilized MCM-41 with two different pore sizes for the delivery of ibuprofen, whose molecular size was in the range of the mesopores. In order to load the OMS, substrates were submerged in a solution of ibuprofen and hexane (33 mg/mL). Upon removal, substrates contained 30 % (w/w) ibuprofen, demonstrating that ibuprofen was absorbed into the mesopores, which was further confirmed by BET analysis. In vitro dissolution analysis of the ibuprofen-loaded OMS exhibited rapid initial release followed by a sustained release, with 80 % release reached after 3 days. This type of two-phase release behavior has been seen across various OMS studies due to the release of the surface adsorbed drug followed by the diffusion of drug from the pores (Thomas et al. 2010); the desorption of drugs in the pores in the presence of water is explained by the affinity OMS has for water over hydrophobic compounds and is diffusion controlled (Mellaerts et al. 2008a, b; Andersson et al. 2004). While the focus of initial studies conducted by Vallet-Regi et al. was on controlled drug-delivery systems, a major focus of OSM research has shifted to immediate release systems for the delivery of poorly water-soluble compounds; this section will highlight the recent work on the use of OMS for the delivery of poorly soluble compounds.

For immediate release applications of OMS materials, the dissolution rate of the drug substance can be tailored by the pore size and surface area. Zhang et al. studied the loading of poorly water-soluble telmisartan (TEL) onto OMS using pore sizes of 4, 8 and 13 nm, obtaining drug loading of 50.7, 61.2 and 60.3 % drug loading (Zhang et al. 2010b). These loading efficiency of the OMS was attributed to the OMS silanol groups forming hydrogen bonding with the drug, albeit weak bonds as seen by the rapid release of the drug from the carrier during in-vitro release testing. The release behavior was consistent with the pore diameter, with 83.5, 95.4 and 100 % release seen at 30 min with increasing pore diameter. Zhang et al. prepared OMS carriers with 28.3 nm pore diameter, also referred to as a mesocellular foam, to increase drug release rate of poorly soluble drug simvastatin (SIM) for 100 % release by 60 min, compared to 62 % from SBA-15 with a 6.5 nm pore diameter (Zhang et al. 2011). Wang et al. showed that the preparation of 3D continuous and interconnected macroporous (pore size 200 and 500 nm) silica particles resulted in faster dissolution of adsorbed indomethacin (IND) when compared to conventional OMS carriers, MCM-41 and SBA-15 OMS. However, this led to reduced physical stability showing recrystallization after 3 months at accelerated stability conditions

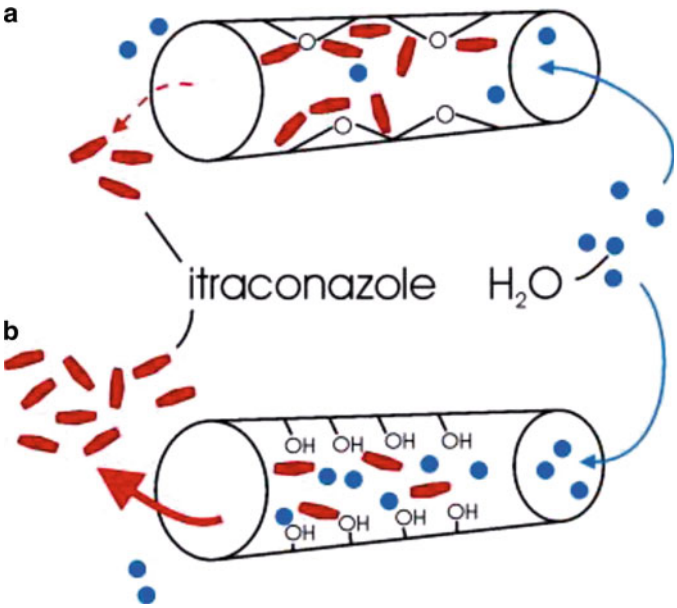

Fig. 13.17 Adsorbed water from humid storage conditions causes hydroxylation of silanol surface, leading to increased release rate of drug upon contact with aqueous fluids. Reproduced with permission from Mellaerts et al. (2010)

(40 °C/75 % RH) (Wang et al. 2013), demonstrating the trade-off between rapid dissolution and physical stability as a function of pore size.

Mellaerts et al. stored itraconazole (ITZ) loaded SBA-15 particles (10 and 20 % w/w drug loading) at 25 °C at 0, 52 and 97 % RH for up to 12 months to determine the long-term stability of adsorbed amorphous ITZ (Mellaerts et al. 2010). Storage at the high humidity (52 and 97 % RH) conditions lead to increased adsorbed water, up to 30 % water content in the 10 % ITZ formulation. The majority of this water was only physically adsorbed, while a small percentage (1.39–1.64 %) was determined to be chemically bound to the SBA-15 surface via hydroxylation. This yielded a faster and more complete release of ITZ from the SBA-15. These changes in drug release were attributed to the hydroxylation of the SBA-15 surface from the bound water, rendering the surface more hydrophilic and more prone to liberating the ITZ when placed in an aqueous environment, as shown in Fig. 13.17. The physical stability of the ITZ was maintained, most probably due to the unchanged or decreasing pore volume that prevented molecular mobility for crystal formation, further emphasizing the benefits of mesoporous materials for use with poorly soluble compounds.

As with amorphous solid dispersion systems, the use of a precipitation inhibitor can be advantageous to maintain supersaturated concentrations. Van Speybroeck et al. was able to show improved maintenance of supersaturation of ITZ in FaSSIF media with the inclusion of HPMC AS and a small improvement with HPMC, when physically mixed with the drug-loaded SBA-15 particles (Van Speybroeck et al. 2010). Interestingly, the improvement from HPMC AS was not seen in-vivo due to

its low solubility at pH < 5.5; however, the HPMC was able to produce a 60 % increase in bioavailability when compared to the OMS (SBA-15)-ITZ alone (AUC_{sum} 14,937 ± 1617 nM h versus 8987 ± 2726 nM h).

Vialpando et al. evaluated the downstream processing of itraconazole (ITZ) loaded OMS in a oral tablet formulation (Vialpando et al. 2011). This study showed that compression of neat OMS and ITZ-loaded OMS resulted in decreased pore volume and surface area due to the collapse of the pore walls which subsequently lead to reduced drug release, particularly at high compression forces. With the addition of microcrystalline cellulose, a plastically deforming filler, and sodium croscarmellose sodium, a disintegrant, there was some recovery of drug release seen when compressed at 120 MPa. In another study, Vialpando et al. evaluated the stability of drug loaded ITZ-OMS particles during a small-scale wet granulation process to improve bulk powder properties (Vialpando et al. 2012). Using a 20 % PVP aqueous solution, granules were prepared without an impact to the OMS pore diameter and volume, indicating physical integrity of the particles. Subsequent compression at 120 MPa compression force did produce a drop in the pore diameter and volume; however, the addition of a disintegrant to the tablet formulation enabled comparable drug release when compared to the granules alone.

In addition to the loading and stabilizing benefits from the nanosized pores of OMS materials, many of these materials are often precipitated as nanosized particles or mesoporous silica nanoparticles (MSN). This offers an obvious advantage to increase cellular uptake, as seen by its early adoption and continuing development for parenteral formulations of cancer drugs and particularly, poorly soluble cancer agents such as paclitaxel (Wang et al. 2015; Meng et al. 2010; Lu et al. 2007; Slowing et al. 2006; Mekaru et al. 2015). Zhang et al. evaluated the use of MSNs for the oral delivery of TEL and showed not only increased cellular uptake when compared to mesoporous silica microparticles (MSM), but also a reduced rate of efflux and thus greater permeability when compared to a control TEL solution (Zhang et al. 2012). This increased permeability correlates well with previous findings of increased permeability of other poorly soluble compounds, such as GRIS, from MSNs (Bimbo et al. 2011). In-vivo studies conducted in beagles (n = 6) showed tablets prepared using ITZ-MSNs and MSMs performed better than the commercial tablet, Micardis®, with relative bioavailabilities of 154.4 and 129.1 %, respectively. This higher bioavailability of the MSN formulation was attributed to the improved absorption of the amorphous TEL from the MSN and the reduced rate of P-gp mediated efflux.

With a high concentration of silanol groups on the mesoporous silica wall surfaces, functionalization with many types of organic molecules to modulate drug-release kinetics is possible, as shown in Fig. 13.18 (Ukmar and Planinšek 2010; Yang et al. 2012). Functionalized OMS systems are especially desirable from a drug delivery standpoint, allowing for targeted release and/or increased protection of the API form harsh biological environments. Researchers have reported the use of a variety of functional moieties for sustained, controlled (Zhang et al. 2010b; Muñoz et al. 2003; Song et al. 2005; Wang et al. 2009; Qu et al. 2006; Tang et al. 2006, 2010; Bernardos et al. 2008; Xu et al. 2008), or pH-dependent release (Peng et al. 2013; Yang et al. 2005). With the addition of an aminopropyl group, Zhang et al. showed that TEL release form OMS could be significantly retarded (Zhang et al.

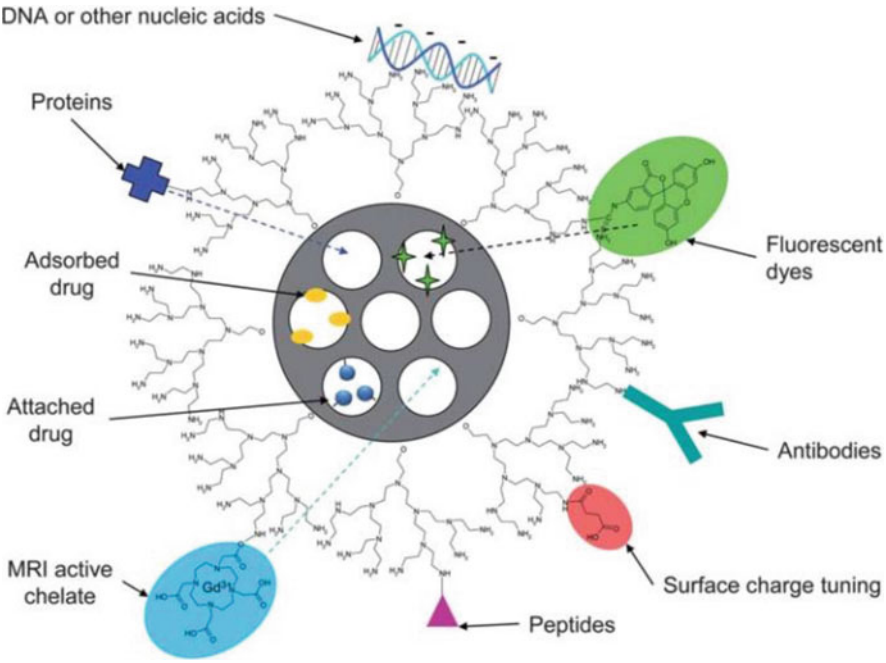

Fig. 13.18 Loading and functionalization possibilities using OMS for drug delivery. Reproduced with permission from Rosenholm et al. (2010)

2010b). The grafted aminopropyl groups exhibited stronger bonding with the TEL than seen with the OMS silanol groups, slowing drug release significantly. In-vitro drug release testing showing 100 % release by 24 h. These results correlate well with previous studies conducted with aminopropyl group modifications to MCM-41 carriers for the delivery of IBU (Muñoz et al. 2003).

As an alternative to the synthesis of OMS materials, existing pharmaceutical grade silicas, i.e. fumed or colloidal silica (Aerosil®) or magnesium aluminum silicate (Neusilin®), have also been utilized as carriers for poorly soluble compounds (Kinnari et al. 2011; Kim 2013). These materials tend to exhibit a more non-ordered structure and can be driven mostly by surface adsorption as opposed to adsorption within the pore walls of the mesostructures previously described; therefore, are often prepared using by adsorption of the poorly soluble compound with a polymer, precipitation inhibitor, and/or solubilizer (Kim 2013). This is the premise of the Spray-dried NanoAdsorbate technology developed by Bend Research®, whereby the dissolved drug and polymer and suspended silica carrier are spray dried to form solid particles with adsorbed amorphous drug-polymer dispersion on the surface of the silica particles. These particles are then amenable for downstream processing, such as encapsulation or tableting.

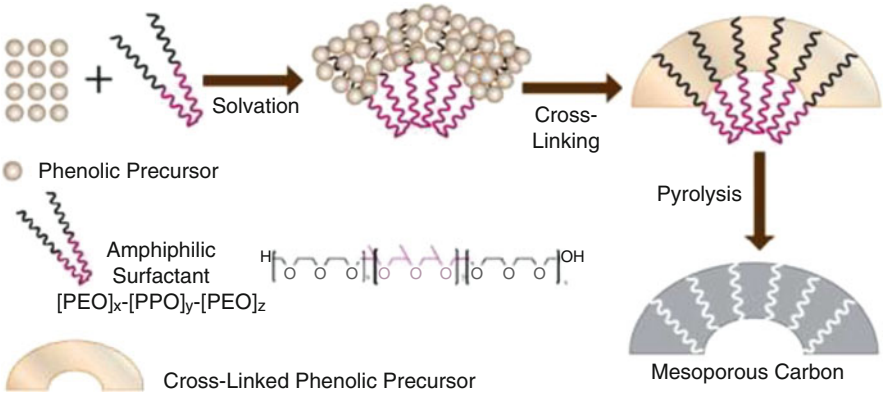

Fig. 13.19 Schematic of soft-templating for the preparation of OMC particles. Reproduced with permission from Saha et al. (2014b)

13.3.1.2 Mesoporous Carbon

The physical liabilities with OMS materials may limit its pharmaceutical application, including the hydroxylation of its silanol groups upon aging and the ease of collapse upon compression. Additionally, safety studies conducted with OMS materials have shown an increased production of reactive oxygen species (ROS), specifically the superoxide $O_2^{\cdot-}$, in Caco-2 cells at a threshold concentration of 1 mg/mL (Heikkilä et al. 2010; Bimbo et al. 2011). Increased levels of ROS can lead to weakened cell membranes, diminished cell metabolism and increased apoptotic signaling. The production of these species was attributed to the silanol groups along the surface of these OMS materials. Based on this, development of inert ordered mesoporous carbon (OMC) materials was initiated for use in drug delivery (Kim et al. 2008; Oh et al. 2010; Saha et al. 2014a). Cytotoxicity studies with OMC materials in Caco-2 cells showed no apparent toxicity at concentrations up to 800 μg/mL (Zhao et al. 2012b). At higher concentrations, cell survival was reduced, although it remained above 80 %, due to carrier agglomeration inside the cell. Studies in HeLa cells also showed positive cell viability for concentrations up to 500 μg/mL, with slight toxicity seen with the highest surface area OMC tested (~70 % survival) at the highest concentration (Gencoglu et al. 2014).

As with OMS, OMC materials are also utilized in other systems and processes, including catalysis and separations. Additionally, porous carbon (or activated charcoal) has been administered to treat acute poisoning in an emergency setting due to its highly absorptive properties (Kulig et al. 1985; Neuvonen and Olkkola 1988; Yachamaneni et al. 2010). The preparation of OMC materials involves hard-templating or soft-templating, also referred to as self-assembly (Liang et al. 2008; Ma et al. 2013). Hard-templating involves preparation of an OMS structure, followed by the incorporation of a carbon source, i.e. sucrose; the particles are then washed to remove the silica template. Soft-templating, shown in Fig. 13.19, involves

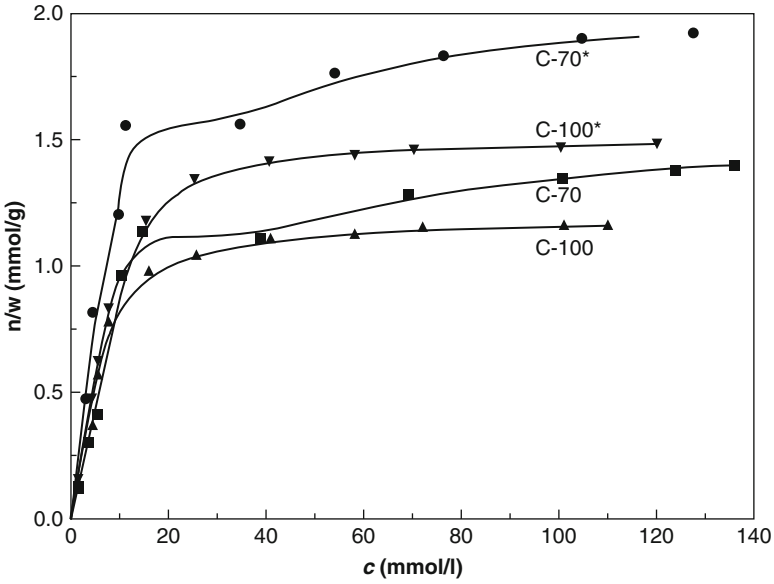

Fig. 13.20 Adsorption isotherms showing IBU solution concentration impact on OMC drug loading with the following sample name (pore diameter, pore volume): C-70 (4.1 nm, 0.97 cm^3/g), C-70 (4.1 nm, 0.97 cm^3/g), C-70* (3.9 nm, 1.42 cm^3/g), C-100 (3.5 nm, 0.64 cm^3/g), C-100* (3.4 nm, 1.11 cm^3/g). Reproduced with permission from Wang et al. (2011a)

cross-linking a suitable organic resin in the presence of pore forming surfactants; suitably those that do not have a char yield. The cross-linking is followed by pyrolysis, which removes the surfactant, and lastly, the carbonization of the matrix. OMC materials have been shown to exhibit larger pore volumes and greater surface areas than their silica counterparts (Zhang et al. 2013).

Wang et al. showed the effect of ibuprofen (IBU) solution concentration and pore volume on OMC drug loading, revealing adsorption isotherms which plateaued as shown in Fig. 13.20, due to saturation of adsorption sites (Wang et al. 2011a). The drug release from the OMC is similar to that of OMS materials in that there is a rapid release of surface adsorbed materials, followed by a slower release of drug from the pores; however, with the absence of the silanol groups, the release of the drug from the OMC carrier is much faster. Zhao et al. evaluated the use of OMC for delivery of a poorly soluble drug, using lovastatin (LOV) as a model compound (Zhao et al. 2012b). 2D hexagonal and 3D cubic structures, also referred to as mesoporous carbon spheres (MCS), of OMC materials were prepared with varying pore sizes and loaded with LOV using a 60 mg/mL organic solvent solution. The 3D cubic material produced higher pore volumes and surface areas than the 2D hexagonal materials. The 3D structure also showed less residual crystallinity of the adsorbed LOV than seen with the 2D cubic materials; however, XPS analysis showed that approximately 53 % of the drug was present on the surface of the 3D structure (10–15 nm depth of analysis), compared to the 38 % on the surface of the

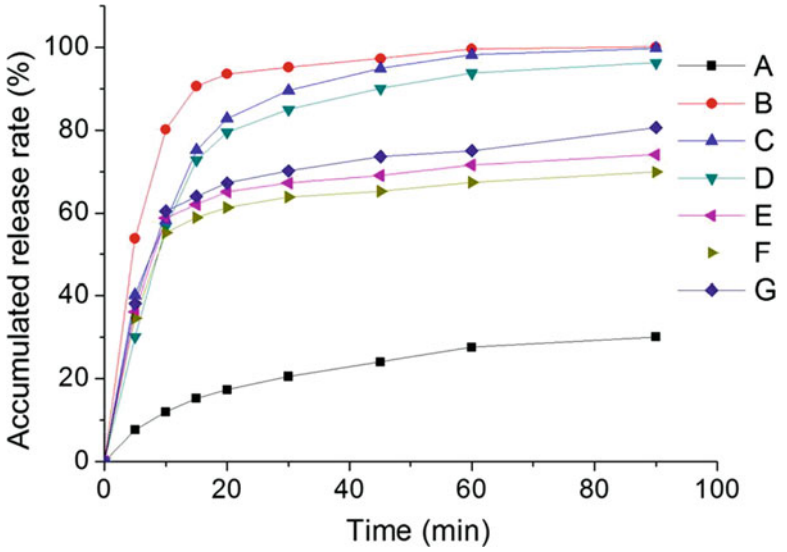

Fig. 13.21 Drug release from pure crystalline LOV (*A*), 3D OMC with pore size 6.0 nm (*B*), 5.1 nm (*C*), 3.8 nm (*D*), and 2D OMC with pore size 5.0 nm (*E*), 4.4 nm (*F*), 7.0 nm (*G*). Reproduced with permission from Zhao et al. (2012b)

Table 13.1 Properties of MSM and c-MCM particles, empty and loaded with CAR. Reproduced with permission from Zhang et al. (2013)

Sample	S_{BET} (m^2/g)	V_t (cm^3/g)	w_{BJH} (nm)	V_{mi} (cm^3/g)	Drug loading (%)
MSMs	893.1 ± 8.5	1.03 ± 0.04	9.1 ± 1.8	0.1 ± 0.02	
c-MCMs	1736.2 ± 13.3	1.82 ± 0.1	7.8 ± 1.9	0.37 ± 0.09	
CAR-MSMs	271.8 ± 9.5	0.36 ± 0.04	3.4 ± 1.5	0	30.1 ± 0.4
CAR-c-MCMs	141.0 ± 23.7	0.15 ± 0.11	2.6 ± 0.3	0	41.6 ± 1.2

2D hexagonal material. The in-vitro drug release, shown in Fig. 13.21, showed rapid release of LOV from the 3D OMC with complete release around 90 min for all pore sizes. The release from the 2D structure showed in initial rapid release, attributed to the surface adsorbed LOV, followed by a slow release of LOV, attributed to release of LOV adsorbed on the pore walls, with only 60–70 % release by 90 min. Although, the rate of release trended with pore size, the small range used (3.8–7.0 nm) provided only small differentiations between the drug release curves.

Zhang et al. utilized carboxylated mesoporous carbon microparticles (c-MCM) to enhance the oral bioavailability of carvedilol (CAR) (Zhang et al. 2013). The carboxylation was incorporated to increase wetting of the MCM upon ingestion. The c-MCMs showed significantly higher pore volume and surface area to MSMs prepared, as shown in Table 13.1, even with only a small difference in pore diameter. These properties enabled a higher drug loading with the c-MCM particles (41.6 %) than with the MSM particles (30.1 %). The c-MSM formulation showed a significant increase in bioavailability in-vivo in beagle dogs against the commercial

Dilatrend® tablet at a 200 mg dose with AUC_{0-24h} of 784.79 ± 56.29 ng h/mL vs. 420.27.2 ± 41.22 ng h/mL of the control. This relative bioavailability of nearly 180 % was attributed to the amorphous state of the CAR, the highly dispersed nature of the drug along the high surface area of the carrier, as well as the limited crystal size restricted by the mesopore size.

In addition to the benefits of increased dissolution, OMC systems can provide other advantages as drug delivery systems. A study conducted using celecoxib (CEL) loaded MCSs with a Caco-2 cell line showed similar suppression of efflux as seen with MSNs (Wang et al. 2014), leading to higher bioavailability. Another study showed reduced mucosa irritation, a side effect of large doses of CEL, when dosed with CEL-OMC attributed to reduced contact of the drug with the mucosal surface as the drug is dispersed on the surface or within the pores of the OMC carrier, as well as the rapid absorption of the small, dispersed amorphous CEL from the carrier (Zhao et al. 2012a).

As with OMS materials, OMC materials can also be functionalized or coated to release drug when triggered by temperature (Zhu et al. 2011), pH (Zhu et al. 2012; Zhang et al. 2015a), applied magnetic field (Oh et al. 2010; Wang et al. 2011b) or other stimuli (Amritha Rammohan et al. 2013), as well as for targeted drug delivery (Zhang et al. 2015b). As the OMC surface does not contain the silanol groups present on OMS surfaces, chemical treatment or activation may be required to introduce functional groups onto the surface for more efficient adsorption and/or functionalization. For example, Saha et al. chemically activated the surface of their OMC materials using KOH to introduce oxygen onto the carbon surface to promote mucoadhesion properties (Saha et al. 2015).

To obtain a sustained release profile and reduce burst release from surface adsorbed drug, Zhang et al. prepared nimeodipine (NIM) loaded OMC with a lipid bilayer or shell (Zhang et al. 2015c). This composite system was able to reduce burst release from 50 to 35 % of drug release within 2 h and extended the release profile to 18 h vs. 12 h for 100 % release when compared to the NIM-OMC alone. Alternatively, for a stimulus based release, Rommohan et al. utilized the slightly negative zeta potential (−0.3 mV) of their OMC particles to facilitate a layer by layer (LbL) polymer coating using positively charged polyelectrolyte, polyethylene imine (PEI), followed by negatively charged polystyrene sulfonates (PSS) and lastly by positively charge polyallylamine hydrochloride (PAH) (Amritha Rammohan et al. 2013). In this system, the drug is released in the presence of high salt concentrations (i.e. 5 M) due to the disruption of electrostatically interacting polymer layers.

For targeted drug delivery, Zhang et al. prepared glucose-based mesoporous carbon nanospheres (MCN) stabilized by phospholipids for increased hydrodynamic stability needed for i.v. administration, as shown in Fig. 13.22 (Zhang et al. 2015b). The particles were able to adsorb a drug loading of 42.7 % of poorly soluble compound SNX-2112, an Hsp90 inhibitor to induce apoptosis (Liu et al. 2012). When compared to a ANX-2112 solution, enhanced antitumor effect was seen with these phospholipid stabilized MCN due to targeting glucose transporters, which are overexpressed in breast cancer cells, for increased cellular uptake and due to the

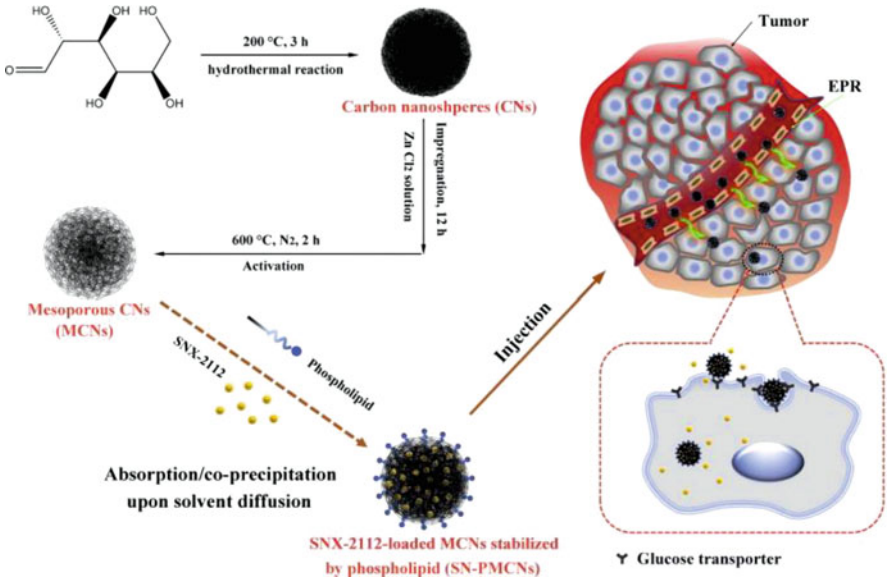

Fig. 13.22 Glucose based MCN stabilized by phospholipids for i.v. administration for targeted drug delivery to tumor site. Reproduced with permission from Zhang et al. (2015b)

nanoparticle size of the carriers which allowed for passive accumulation due to the enhanced permeation and retention (EPR) effect seen with the leaky vasculature in tumor tissues, also shown in Fig. 13.22.

13.3.1.3 Other Mesoporous Materials

The evaluation of alternative mesoporous materials has also gained interest for drug delivery. Inorganic mesoporous carriers have included hydroxycarbonate apatite and titanium dioxide (Jiang et al. 2012). Organic mesoporous carriers have included starch and porous polymers, such as PVA (Roberts and Zhang 2013; Wu et al. 2011).

Hydroxycarbonate apatite (HCA) is another material commonly employed for tissue and bone engineering scaffolds. HCA is a calcium phosphate-based inorganic material that has often been used as artificial bone materials. Its inert nature, biocompatibility, relatively high surface area and uniform pore formation has led to the adoption of HCA and hydroxyapatite (HA) as drug delivery systems (Zhang et al. 2010a; Zhao et al. 2012c; Ye et al. 2010; Mizushima et al. 2006). Zhao et al. prepared mesoporous HCA particles using a hard-template method with $CaCO_3$ as the sacrificial template and CTAB as the pore-forming agent (Zhao et al. 2012c). The particles with the largest pore volume and surface area (0.175 mL/g and 121.9 m^2/g, respectively) were then loaded with CAR using carrier to drug ratios of 3:1, 2:1, and 1:1 to obtain drug loading of 23, 31, and 48 %, respectively; however,

the higher drug load particles (31 and 48 %) showed a higher degree of residual crystallinity. The 23 % drug loaded formulation showed a faster and more complete drug release with over 90 % release seen by 20 min when compared to the other drug loads and raw drug, attributed to higher degree of amorphous CAR on the lower drug loaded formulation. The 23 % drug loaded particles were also shown to be physically stable for when held in a desiccator at 25 °C for 6 months; however, as FTIR analysis showed no physical interaction, the stability of the adsorbed drug was attributed to the inhibition of recrystallization by the restrictive pore size.

Porous starch has been used for tissue engineering and bone cements due their biocompatible and biodegradable nature (Gomes et al. 2001, 2002). Additionally, the availability of hydroxyl groups on the surface of starch enables interactions for adsorption and/or functionalization. Porous starch can be prepared by various techniques, including injection molding, in-situ polymerization, or using a solvent-exchange method to produce a porous gel (Nakamatsu et al. 2006). Wu et al. evaluated those use of porous starch as a carrier for poorly soluble drug, LOV (Wu et al. 2011). Although the large and irregular pore diameters, 20–80 nm, resulted in adsorbed LOV present in a partially amorphous form, the dissolution rates were still faster than the commercially available capsules.

13.3.2 Co-amorphous Mixtures

The amorphous state of a drug is a high-energy, highly disordered state that enables higher apparent solubility and a faster dissolution rate than its crystalline form (Hancock and Zografi 1997). However, this is a metastable form that has a tendency to crystallize during manufacture, storage, or during drug release. ASDs using polymer carriers have become a preferred method to enhance solubility and bioavailability of poorly soluble compounds utilized in several marketed products including Sporanox®, Kaletra®, and Incivek®. In these polymer-based systems, the drug is molecularly dispersed in a polymer carrier and can be kinetically stabilized by high T_g and/or high viscosity polymers to reduce molecular mobility. Additionally, chemical bonding between the polymer and drug can lead to additional stabilization (Janssens and Van den Mooter 2009; Laitinen et al. 2013). One of the limitations of polymer-based solid dispersions is the high weight percentage of polymer that is often needed to form a molecular dispersion or glassy solution; this can lead to a higher pill burden for drugs that require higher doses. Additionally, many of the polymer carriers used require a plasticizer for processing and/or are hygroscopic; plasticizer and adsorbed water, which has a plasticizing effect, can lower the system T_g, leading to physical instability. Co-amorphous systems, defined as a combination of two small molecules, have been found to increase apparent solubility and dissolution rate, as well as maintain physical stability with drug-small molecule ratios of 1:2, 1:1, and 2:1 (Allesø et al. 2009; Chieng et al. 2009; Löbmann et al. 2011, 2012; Dengale et al. 2014; Knapik et al. 2015; Teja et al. 2015), making them a promising alternative to the conventional polymer-based amorphous dispersion. Many of these co-amorphous systems have been prepared using sugars, urea, and citric acid (Lu

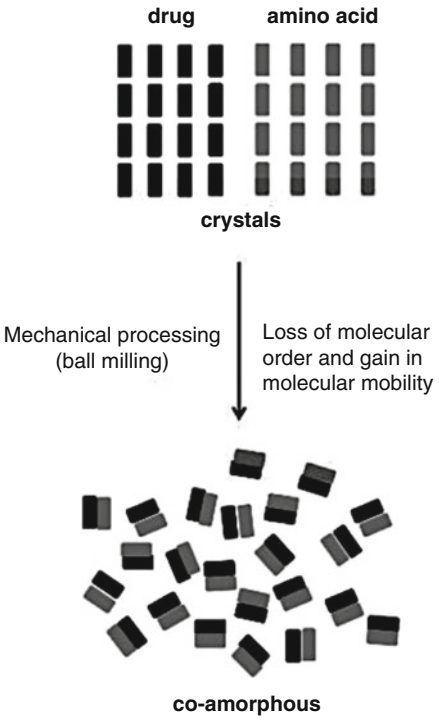

Fig. 13.23 Preparation of co-amorphous drug-amino acid via milling. Reproduced with permission from Jensen et al. (2015b)

and Zografi 1998; Ahuja et al. 2007; Masuda et al. 2012; Ewing et al. 2015); however, much of the research has focused on the use of drug-drug and drug-amino acid mixtures (Löbmann et al. 2014). Preparation of these co-amorphous mixtures involves conventional manufacturing methods, such as co-milling, shown in Fig. 13.23, or solvent evaporation methods, including spray drying.

13.3.2.1 Co-amorphous Drug-Drug Mixtures

First published investigations of co-amorphous mixtures were as early as 1989, with the preparation of phenobarbital-salicin and phenobarbital-antipyrine binary systems (Fukuoka et al. 1989). Both systems showed resulting T_gs that correlated well with theoretical values calculated by the Gordon-Taylor equation, which presumes no interaction between the two components. However, solid state characterization of other systems, including cimetidine (CIM)-naproxen (NAP) co-amorphous mixtures exhibited T_gs higher than the Gordon-Taylor prediction, suggesting an interaction between the imidazole ring of the CIM with the carboxyl group of the NAP, which may contribute to the formation and stability of the mixture (Yamamura et al. 1996; Allesø et al. 2009). This interaction was also seen with a CIM- indomethacin (IND) mixture (Yamamura et al. 2000), while a CIM-diflunisil mixture showed a stronger interaction, forming an amorphous salt (Yamamura et al. 2002).

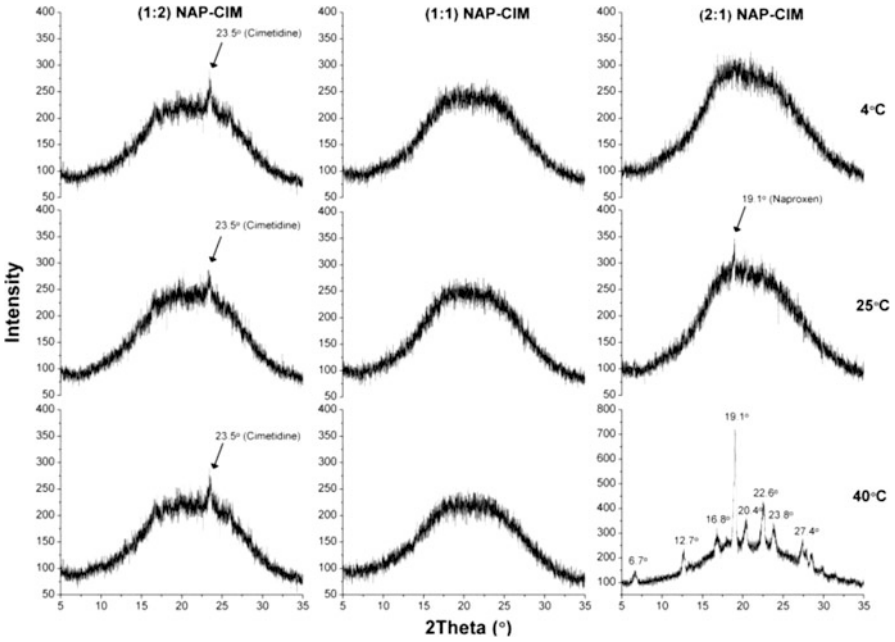

Fig. 13.24 PXRD diffractograms of CIM-NAP co-amorphous mixtures prepared at varying ratios after 33 days of storage in desiccators at 4, 25, and 40 °C. Reproduced with permission from Allesø et al. (2009)

Alesso et al. further evaluated the CIM-NAP co-amorphous mixture prepared by co-milling, in place of the solvent evaporation methods from the previous studies. These studies showed that milling of NAP alone was not sufficient to produce amorphous NAP; however, co-milling with CIM produced co-amorphous mixtures at 1:2, 1:1, and 2:1 NAP-CIM. Of these, only the 1:1 ratio was found to be physically stable, as shown in Fig. 13.24, attributed to the 1:1 molecular interaction between the two drug molecules.

In another system, also prepared by co-milling, IND with ranitidine hydrochloride (RAN) formed a co-amorphous mixtures, with the 1:1 ratio showing a higher degree of physical stability after 30 days than the 1:2 and 2:1 IND-RAN mixtures on stability, although all showed some degree of recrystallization when held at 40 °C (Chieng et al. 2009). As with the phenobarbital-salicin and phenobarbital-antipyrine co-amorphous mixtures, the IND-RAN mixture T_gs correlated well with predicted values, indicating no chemical interaction. FTIR analysis showed some interaction between the carboxylic acid of the IND with the imine group (C=N) of the RAN; however, these interactions were not strong enough to form a salt or co-crystal.

IND was also evaluated with NAP and again showed that the presence of IND enabled the formation of co-amorphous IND-NAP, even when amorphous NAP could not be prepared alone (Löbmann et al. 2011). It was theorized that the IND-NAP formed a heterodimer though hydrogen bonding between the each drug's car-

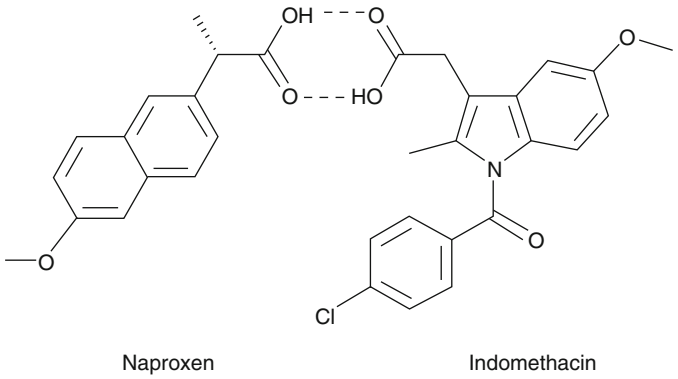

Fig. 13.25 Chemical structures and proposed mechanism of interaction between IND and NAP. Reproduced with permission from Löbmann et al. (2011)

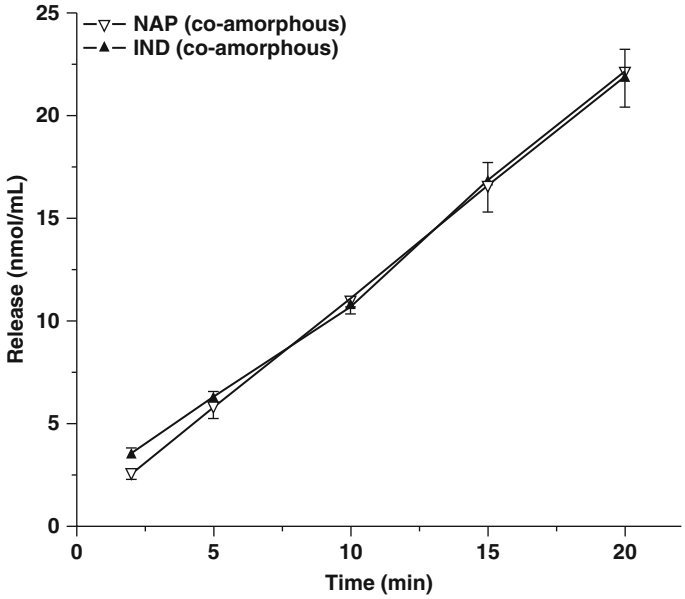

Fig. 13.26 Intrinsic drug release of co-amorphous IND-NAP (1:1) showing synchronized release of both drugs. Reproduced with permission from Löbmann et al. (2011)

boxylic group, as shown in Fig. 13.25; this was later confirmed using IR and quantum mechanical calculations (Löbmann et al. 2013b). Predicted T_g values, assuming no interaction, deviated for the experimentally determined values; however, when the 1:1 drug ratio was inserted as an individual component (assuming interaction) with excess drug representing the second compound, the 1:2 and 2:1 predicted T_g values matched the experimentally determined values. The intrinsic dissolution rate (IDR) testing of the 1:1 IND-NAP mixture showed synchronous release, shown in

Fig. 13.26, with both drugs showing increased drug release rates than their crystalline counterparts (NAP: 0.30–0.41 mg/cm^2 min; IND: 0.055–0.42 mg/cm^2 min). IND also showed an improvement over amorphous IND alone (0.36 mg/cm^2 min); this finding is counter to previous reports of decreased drug release in the presence of another amorphous compound (Trasi and Taylor 2015). Increased saturation solubility was also seen with talinolol (TLN) in a TLN: naringin (NRG) co-amorphous mixture when compared to the amorphous TLN alone (Teja et al. 2015).

IND-Ritonavir (RTV) co-amorphous mixtures showed good correlation with predicted T_g and no evidence of bonding via FTIR analysis, indicating no heterodimer formation as seen with IND: NAP mixtures (Dengale et al. 2014). Dengale et al. showed this system to be stable for 90 days with all ratios studied, 1:2, 1:1, and 2:1, and stability was attributed to the miscibility of the drug-drug mixture. Notably, even with threefold increase in the solubility of both drugs, only the RTV dissolution rate was significantly enhanced from the co-amorphous dispersion.

In another study, ezetimib (EZB)-indapamid (IDP) co-amorphous mixtures were made at ratios varying from 10:1 to 1:2 to evaluate physical stability in the absence of any significant molecular interaction (Knapik et al. 2015). In this particular mixture, the EZB:IDP (10:1) was found to be stable for 72 days at room temperature when prepared with a low level of IDP; this was attributed to an anti-plasticizing effect by the IDP on the EZB. It should be noted that the stability studies conducted with these co-amorphous mixtures were done in dry conditions, so the effect of humidity on physical stability is yet to be reported. Although the exact mechanism of formation and stabilization of these co-amorphous mixtures are not fully understood, the intimate molecular mixing and interactions between the two molecules, even if they are weak interactions, are considered barriers to prevent recrystallization (Grohganz et al. 2013).

13.3.2.2 Co-amorphous Drug-Amino Acid Mixtures

Although, drug-drug co-amorphous mixtures for FDC products may be advantageous in some cases, co-amorphous mixtures using an inactive small molecule offer an alternative for monotherapy applications. Mura et al. showed the ability of arginine (ARG) to form strong interactions with NAP, produce a mostly amorphous system upon grinding, and exhibit enhanced dissolution properties (Mura et al. 2003, 2005); thus, opening the door to the use of amino acids as an inactive small molecule for co-amorphous formulations. Amino acids, consisting of both an amine and carboxylic group, have previously been utilized as salt-formers to improve drug solubility (Bastin et al. 2000; Hirano et al. 2010). As they are organic molecules, crucial to protein synthesis and other biological processes, they are inherently biocompatible (Dutta and Dey 2011). Furthermore, amino acids can facilitate enhanced and/or targeted drug delivery from increased permeability and cellular uptake due to amino acid transporters along the cellular membrane, particularly when those transporters are upregulated as seen with cancer cells (Tsume et al. 2011; Bhutia et al. 2015; Gynther et al. 2008; Maeng et al. 2014).

Löbmann et al. screened formulations utilizing carbamazepine (CBZ) and IND and amino acids ARG, phenylalanine (PHE), tryptophan (TRP), and tyrosine (TYR) at 1:1 and 1:1:1 ratios of drug: amino acid or drug: amino acid: amino acid (Löbmann et al. 2013a). The amino acids were chosen based on the binding site of the biological receptors of the respective drugs, ARG and TYR for IND binding to COX-2 and PHE and TRP for CBZ binding to neuronal Na+ channels; however, formulations were made for each drug using all four amino acids by co-milling. Calculated solubility parameters for CBZ, IND and the four amino acids were not significantly different with a range of 24.9 MPa (CBZ) to 30.6 MPa (TRP), indicating good miscibility. Co-amorphous mixtures were formed with IND with ARG, PHE and TRP, as well as 1:1:1 ratios with PHE:TRP and ARG-PHE. CBZ was only able to form co-amorphous mixtures with TRP and PHE:TRP and ARG:TRP; additionally, amorphous CBZ was unable to be prepared by milling. All of the co-amorphous mixtures exhibited higher T_g values than the amorphous drug alone (CBZ was prepared by quench cooling for this analysis), showing the ability to improve physical stability of the amorphous API by increasing the mixture T_g. The mixtures were shown to be physically stable for 6 months at room temperature, while the amorphous IND and CBZ recrystallized within 1 week, further supporting the stabilizing effect of the amino acid. The mechanism of stabilization was also attributed to the molecular mixing and interactions seen using FTIR analysis (Löbmann et al. 2013c).

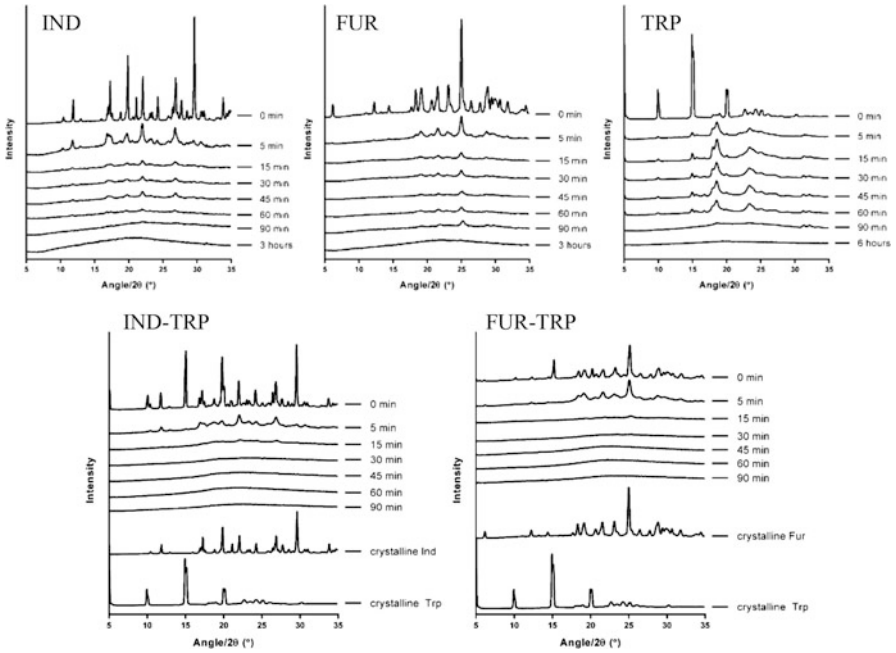

Fig. 13.27 PXRD diffractograms of milled IND, FUR, and TRP (*top*) and 1:1 IND-TRP and 1:1 FUR-TRP mixtures (*bottom*) as a function of milling time. Reproduced with permission from Jensen et al. (2015b)

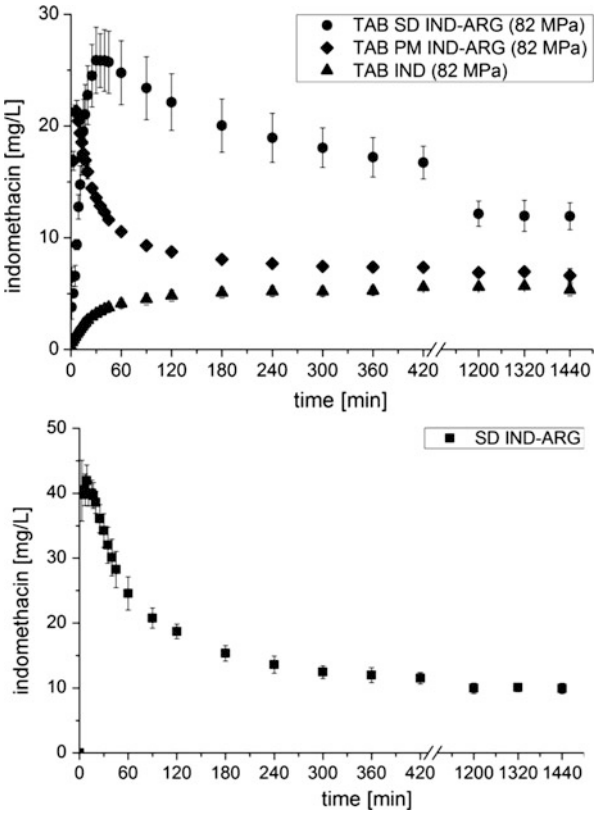

Fig. 13.28 Drug release (*top*) from tablets containing spray-dried (SD) IND–ARG, PM IND–ARG or crystalline IND prepared with 50 mg IND at compaction pressures of 82 MPa and (*bottom*) SD IND-ARG powder in 900 mL phosphate buffer pH 4.5 (non-sink), 50 rpm USP II paddle speed. Reproduced with permission from Lenz et al. (2015)

However, this screening showed that it was is not necessarily predictable as to which amino acids could form co-amorphous mixtures with which drug substance solely based on receptor binding properties. These results are in line with results found from another study, showing SIM and glibenclamide (GBC) co-amorphous mixture with and without a receptor amino acid (Laitinen et al. 2014).

Jensen et al. showed the formation of the co-amorphous mixtures as a function of milling time, further demonstrating the ability of the two small molecules to facilitate conversion to amorphous of molecules that cannot otherwise be readily converted to the amorphous state upon milling (Jensen et al. 2015b). Figure 13.27 shows that milling of individual components, IND, furosemide (FUR) and amino acid, TRP, was unable to produce completely amorphous material within 90 min of milling; however, with the mixtures, significant reduction in crystallinity was seen after 5 min, with complete co-amorphous formation by 30 min.

Spray-drying has been demonstrated as a more scalable process to prepare co-amorphous drug-amino acid mixtures (Jensen et al. 2015a; Lenz et al. 2015). Lenz et al. also evaluated the impact of tableting spray-dried co-amorphous mixtures on release properties and release, using an IND-ARG co-amorphous formulation. When compared to a tablet containing crystalline IND and physical mixture (PM)

of crystalline IND and ARG, the IND-ARG co-amorphous tablet showed a longer maintenance of supersaturation, as shown in Fig. 13.28. Although, the release rate from the tablet was slower than the neat spray-dried powder, also shown in Fig. 13.28, this seems to be advantageous for the maintenance of supersaturation. Surprisingly, the PM formulation showed in-situ formation of IND-ARG salt that lead to a high degree of supersaturation; however, it was also quicker to recrystallize in solution, with final concentrations near that of the crystalline IND.

Overall, these co-amorphous mixtures provide a promising alternative formulation techniques for creating and stabilizing amorphous drug for enhanced bioavailability. Although the mechanism of formation and stabilization is not completely understood, it is presumed that the increase in T_g, molecular mixing, and/or molecular interactions, from hydrogen and π-π interactions to the formation of co-crystals or salts, contribute to the inhibition of recrystallization.

13.4 Summary

A number of techniques have emerged in recent years that have applications in the formulation of poorly water-soluble compounds. However, selection of a suitable processing or formulation technique is highly dependent on the specific physicochemical properties of the drug substance being studied, as well as the target release properties. Many drug substances exhibit instabilities or other properties that severely limit the number of feasible formulation and processing techniques. The emerging technologies described in this chapter offer specific advantages over traditional processing and formulation techniques, which may allow certain drugs to be formulated that would otherwise not be possible.

Method Capsule 1

Preparation of Solid Dispersions: KinetiSol® Dispersing
Based on the method reported by DiNunzio et al. (2010b)

Objective

- To rapidly prepare plasticizer-free solid dispersions containing Eudragit® L100-55

Equipment and Reagents

- Eudragit® L100-55
- Itraconazole
- Liquid nitrogen
- KinetiSol® Dispersing Compounder
- Impact mill
- 60-mesh screen

Method

- Input an ejection temperature of 158 °C and a rotational speed of 3000 rpm into the control module.
- Mix a 1:2 blend of itraconazole:Eudragit® L100-55 in a polyethylene bag for 1-min.
- Charge the blended material into the processing chamber.
- Pre-cool steel plates with liquid nitrogen.
- Start the compounding process.
- Using the data-acquisition system, monitor temperature and rotational speeds.
- After material is discharged, quench between chilled plates.
- Grind the brittle material in an impact mill and pass through a 60-mesh screen.

Results

- The temperature of the blend reached 158 °C in 14.1 s with exposure to temperatures greater than 100 °C for only 2 s, resulting in no chemical degradation of Eudragit® L100-55.
- X-ray powder diffraction patterns indicated that the composition was amorphous.
- Differential scanning calorimetry thermograms showed the presence of a single-phase system with no endothermic events.
- The plasticizer-free composition exhibited a high degree of physical stability due to its high glass transition temperature.

Method Capsule 2

Preparation of Solid Dispersions: Electrostatic Spinning
Based on the method reported by Verreck et al. (2003a)

Objective

- To prepare solid dispersions of itraconazole by electrostatic spinning

Equipment and Reagents

- Hypromellose
- Itraconazole
- Ethanol
- Methylene chloride
- Electrostatic spinner
- Turbula mixer
- Cryogenic mill
- Liquid nitrogen

Method

- Prepare physical blends containing 20 % w/w or 40 % w/w itraconazole by mixing in a Turbula mixer for 10 min
- Prepare a 12 % w/w solution of the itraconazole: hypromellose blend in a mixture of ethanol and methylene chloride (40:60 ethanol: methylene chloride w/w)
- Place the solution into the spinneret and apply a high voltage (16–24 kV)
- *Optional*: Mill the resulting fibers by cryogenic grinding

Results

- SEM analysis demonstrated that drug concentration and processing voltage can significantly impact fiber size and shape.
- Differential scanning calorimetry thermograms showed that compositions containing 20 % (w/w) and 40 % (w/w) itraconazole were amorphous.
- Differential scanning calorimetry thermograms indicated that the milling process facilitated recrystallization of amorphous itraconazole.
- Dissolution rates of itraconazole were found to be highly dependent on the drug: polymer ratio, fiber diameter, and presentation used (nonwoven fabrics, milling, etc.).

Method Capsule 3

Preparation of Solid Dispersions: Mesoporous Silica
Based on the method reported by Mellaerts et al. (2008b)

Objective

- To prepare mesoporous silica loaded with itraconazole

Equipment and Reagents

- Itraconazole
- Ordered mesoporous silica (OMS)
- Methylene chloride
- Rotary mixer

Method

- Prepare a 5 mg/mL solution of itraconazole in methylene chloride.
- Add OMS at a OMS:Itraconazole ratio of 75:25 and agitate for 24 h with a rotary mixer.
- Remove methylene chloride by evaporation and dry powder overnight at 35 °C.
- Heat mixture to 100 °C for 5 min under vacuum and at 40 °C for 48 h to ensure complete removal of methylene chloride.

Results

- Differential scanning calorimetry thermograms did not exhibit glass transition or endothermic events, indicating that itraconazole was molecularly dispersed within the OMS.
- BET analysis showed that the surface area of OMS decreased from 844 to 355 m^2/g after loading with itraconazole.
- Dissolution studies demonstrated that release rates of itraconazole from OMS were significantly faster than crystalline itraconazole.
- Bioavailability of itraconazole-loaded OMS was found to be similar to that of the marketed product, Sporanox®.

References

Ahuja N, Katare OP, Singh B (2007) Studies on dissolution enhancement and mathematical modeling of drug release of a poorly water-soluble drug using water-soluble carriers. Eur J Pharm Biopharm 65(1):26–38

Allesø M, Chieng N, Rehder S, Rantanen J, Rades T, Aaltonen J (2009) Enhanced dissolution rate and synchronized release of drugs in binary systems through formulation: amorphous naproxen–cimetidine mixtures prepared by mechanical activation. J Control Release 136(1):45–53

Alomari M, Mohamed FH, Basit AW, Gaisford S (2015) Personalised dosing: printing a dose of one's own medicine. Int J Pharm 494(2):568–577. doi:10.1016/j.ijpharm.2014.12.006

Amritha Rammohan B, Tayal L, Kumar A, Sivakumar S, Sharma A (2013) Fabrication of polymer-modified monodisperse mesoporous carbon particles by template-based approach for drug delivery. RSC Adv 3(6):2008–2016. doi:10.1039/C2RA22261B

Andersson J, Rosenholm J, Areva S, Lindén M (2004) Influences of material characteristics on ibuprofen drug loading and release profiles from ordered micro-and mesoporous silica matrices. Chem Mater 16(21):4160–4167

Baldoni JM, Ignatious F, Inventors (2001) Electrospun pharmaceutical compositions patent WO2001054667

Balogh A, Drávavölgyi G, Faragó K, Farkas A, Vigh T, Sóti PL et al (2014) Plasticized drug-loaded melt electrospun polymer mats: characterization, thermal degradation, and release kinetics. J Pharm Sci 103(4):1278–1287. doi:10.1002/jps.23904

Balogh A, Farkas B, Faragó K, Farkas A, Wagner I, Van Assche I et al (2015) Melt-blown and electrospun drug-loaded polymer fiber mats for dissolution enhancement: a comparative study. J Pharm Sci 104(5):1767–1776. doi:10.1002/jps.24399

Bastin RJ, Bowker MJ, Slater BJ (2000) Salt selection and optimisation procedures for pharmaceutical new chemical entities. Org Process Res Dev 4(5):427–435. doi:10.1021/op000018u

Bennett RC, Brough C, Miller DA, O'Donnell KP, Keen JM, Hughey JR et al (2013) Preparation of amorphous solid dispersions by rotary evaporation and KinetiSol dispersing: approaches to enhance solubility of a poorly water-soluble gum extract. Drug Dev Ind Pharm 41(3):382–397

Bernardos A, Aznar E, Coll C, Martínez-Mañez R, Barat JM, Marcos MD et al (2008) Controlled release of vitamin B 2 using mesoporous materials functionalized with amine-bearing gate-like scaffoldings. J Control Release 131(3):181–189

Bhardwaj N, Kundu SC (2010) Electrospinning: a fascinating fiber fabrication technique. Biotechnol Adv 28(3):325–347. doi:10.1016/j.biotechadv.2010.01.004

Bhutia YD, Babu E, Ramachandran S, Ganapathy V (2015) Amino acid transporters in cancer and their relevance to "Glutamine Addiction": novel targets for the design of a new class of anticancer drugs. Cancer Res 75(9):1782–1788. doi:10.1158/0008-5472.can-14-3745

Bimbo LM, Mäkilä E, Laaksonen T, Lehto V-P, Salonen J, Hirvonen J et al (2011) Drug permeation across intestinal epithelial cells using porous silicon nanoparticles. Biomaterials 32(10):2625–2633

Boehm RD, Miller PR, Hayes SL, Monteiro-Riviere NA, Narayan RJ (2011) Modification of microneedles using inkjet printing. AIP Adv 1(2):22139. doi:10.1063/1.3602461

Bradbury MS, Pauliah M, Wiesner U (2015) Ultrasmall fluorescent silica nanoparticles as intraoperative imaging tools for cancer diagnosis and treatment. In: Fong Y, Giulianotti PC, Lewis J, Groot Koerkamp B, Reiner T (eds) Imaging and visualization in the modern operating room. Springer, New York, pp 167–179

Breitenbach J (2002) Melt extrusion: from process to drug delivery technology. Eur J Pharm Biopharm 54(2):107–117

Brough C, Miller D, Keen J, Kucera S, Lubda D, Williams R III (2015) Use of polyvinyl alcohol as a solubility-enhancing polymer for poorly water soluble drug delivery (part 1). AAPS PharmSciTech 17(1):1–13. doi:10.1208/s12249-015-0458-y

Campbell I, Bourell D, Gibson I (2012) Additive manufacturing: rapid prototyping comes of age. Rapid Prototyping J 18(4):255–258. doi:10.1108/13552541211231563

Capone C, Di Landro L, Inzoli F, Penco M, Sartore L (2007) Thermal and mechanical degradation during polymer extrusion processing. Polym Eng Sci 47(11):1813–1819

Chieng N, Aaltonen J, Saville D, Rades T (2009) Physical characterization and stability of amorphous indomethacin and ranitidine hydrochloride binary systems prepared by mechanical activation. Eur J Pharm Biopharm 71(1):47–54

Chiou WL, Riegelman S (1971) Pharmaceutical applications of solid dispersion systems. J Pharm Sci 60(9):1281–1302

Chua CK, Leong KF, An J (2014) Introduction to rapid prototyping of biomaterials. In: Narayan R (ed) Rapid prototyping of biomaterials. Woodhead Publishing, Philadelphia, pp 1–15

Coppens K, Hall M, Larsen P, Mitchell S, Nguyen P, Read M et al (eds) (2004) Thermal and rheological evaluation of pharmaceutical excipients for hot melt extrusion. AAPS annual meeting and exposition, Baltimore, MD

Crowley MM, Zhang F, Koleng JJ, McGinity JW (2002) Stability of polyethylene oxide in matrix tablets prepared by hot-melt extrusion. Biomaterials 23(21):4241–4248. doi:10.1016/S0142-9612(02)00187-4

Crowley MM, Zhang F, Repka MA, Thumma S, Upadhye SB, Kumar Battu S et al (2007) Pharmaceutical applications of hot-melt extrusion: part I. Drug Dev Ind Pharm 33(9):909–926

Daly R, Harrington TS, Martin GD, Hutchings IM (2015) Inkjet printing for pharmaceutics—a review of research and manufacturing. Int J Pharm 494(2):554–567. doi:10.1016/j.ijpharm.2015.03.017

De Jaeghere W, De Beer T, Van Bocxlaer J, Remon JP, Vervaet C (2015) Hot-melt extrusion of polyvinyl alcohol for oral immediate release applications. Int J Pharm 492(1–2):1–9. doi:10.1016/j.ijpharm.2015.07.009

Deitzel J, Kleinmeyer J, Harris D, Tan NB (2001) The effect of processing variables on the morphology of electrospun nanofibers and textiles. Polymer 42(1):261–272

Dengale SJ, Ranjan OP, Hussen SS, Krishna BSM, Musmade PB, Gautham Shenoy G et al (2014) Preparation and characterization of co-amorphous Ritonavir–Indomethacin systems by solvent evaporation technique: improved dissolution behavior and physical stability without evidence of intermolecular interactions. Eur J Pharm Sci 62:57–64. doi:10.1016/j.ejps.2014.05.015

Dimov SS (2001) Rapid manufacturing: the technologies and applications of rapid prototyping and rapid tooling. Springer, London

DiNunzio JC, Brough C, Brown A, Williams RO, McGinity JW (2008). Fusion processing of itraconazole and griseofulvin solid dispersions by a novel high energy manufacturing technology—KinetiSol® dispersing. American Association of Pharmaceutical Scientists Annual Meeting; Atlanta, Georgia

DiNunzio JC, Brough C, Hughey JR, Miller DA, Williams RO III, McGinity JW (2010a) Fusion production of solid dispersions containing a heat-sensitive active ingredient by hot melt extrusion and Kinetisol® dispersing. Eur J Pharm Biopharm 74(2):340–351. doi:10.1016/j.ejpb.2009.09.007

DiNunzio JC, Brough C, Miller DA, Williams RO III, McGinity JW (2010b) Applications of KinetiSol® Dispersing for the production of plasticizer free amorphous solid dispersions. Eur J Pharm Sci 40(3):179–187. doi:10.1016/j.ejps.2010.03.002

DiNunzio JC, Brough C, Miller DA, Williams RO, McGinity JW (2010c) Fusion processing of itraconazole solid dispersions by Kinetisol® dispersing: a comparative study to hot melt extrusion. J Pharm Sci 99(3):1239–1253. doi:10.1002/jps.21893

DiNunzio JC, Hughey JR, Brough C, Miller DA, Williams RO III, McGinity JW (2010d) Production of advanced solid dispersions for enhanced bioavailability of itraconazole using KinetiSol® dispersing. Drug Dev Ind Pharm 36(9):1064–1078

Doshi J, Reneker DH (eds) (1993) Electrospinning process and applications of electrospun fibers. Industry Applications Society annual meeting. Conference record of the 1993 IEEE, IEEE

Dutta P, Dey J (2011) Drug solubilization by amino acid based polymeric nanoparticles: characterization and biocompatibility studies. Int J Pharm 421(2):353–363. doi:10.1016/j.ijpharm.2011.10.011

El'Darov E, Mamedov F, Gol'Dberg V, Zaikov G (1996) A kinetic model of polymer degradation during extrusion. Polym Degrad Stab 51(3):271–279

Ewing AV, Biggart GD, Hale CR, Clarke GS, Kazarian SG (2015) Comparison of pharmaceutical formulations: ATR-FTIR spectroscopic imaging to study drug-carrier interactions. Int J Pharm 495(1):112–121. doi:10.1016/j.ijpharm.2015.08.068

Fadeel B, Garcia-Bennett AE (2010) Better safe than sorry: understanding the toxicological properties of inorganic nanoparticles manufactured for biomedical applications. Adv Drug Deliv Rev 62(3):362–374. doi:10.1016/j.addr.2009.11.008

Follonier N, Doelker E, Cole ET (1994) Evaluation of hot-melt extrusion as a new technique for the production of polymer-based pellets for sustained release capsules containing high loadings of freely soluble drugs. Drug Dev Ind Pharm 20(8):1323–1339

Fousteris E, Tarantili PA, Karavas E, Bikiaris D (2013) Poly (vinyl pyrrolidone)–poloxamer-188 solid dispersions prepared by hot melt extrusion. J Therm Anal Calorim 113(3):1037–1047

Fukuoka E, Makita M, Yamamura S (1989) Glassy state of pharmaceuticals. III: Thermal properties and stability of glassy pharmaceuticals and their binary glass systems. Chem Pharm Bull 37(4):1047–1050. doi:10.1248/cpb.37.1047

Garcia-Bennett AE, Che S, Miyasaka K, Sakamoto Y, Ohsuna T, Liu Z et al (2005) Studies of anionic surfactant templated mesoporous structures by electron microscopy. In: Abdelhamid S, Mietek J (eds) Studies in surface science and catalysis. Elsevier, Amsterdam, pp 11–18

Gencoglu MF, Spurri A, Franko M, Chen J, Hensley DK, Heldt CL et al (2014) Biocompatibility of soft-templated mesoporous carbons. ACS Appl Mater Interfaces 6(17):15068–15077. doi:10.1021/am503076u

Ghebremeskel A, Vemavarapu C, Lodaya M (2006) Use of surfactants as plasticizers in preparing solid dispersions of poorly soluble API: stability testing of selected solid dispersions. Pharm Res 23(8):1928–1936. doi:10.1007/s11095-006-9034-1

Gomes ME, Ribeiro AS, Malafaya PB, Reis RL, Cunha AM (2001) A new approach based on injection moulding to produce biodegradable starch-based polymeric scaffolds: morphology, mechanical and degradation behaviour. Biomaterials 22(9):883–889. doi:10.1016/S0142-9612(00)00211-8

Gomes ME, Godinho JS, Tchalamov D, Cunha AM, Reis RL (2002) Alternative tissue engineering scaffolds based on starch: processing methodologies, morphology, degradation and mechanical properties. Mater Sci Eng C 20(1–2):19–26. doi:10.1016/S0928-4931(02)00008-5

Goyanes A, Buanz ABM, Hatton GB, Gaisford S, Basit AW (2015a) 3D printing of modified-release aminosalicylate (4-ASA and 5-ASA) tablets. Eur J Pharm Biopharm 89:157–162. doi:10.1016/j.ejpb.2014.12.003

Goyanes A, Wang J, Buanz A, Martínez-Pacheco R, Telford R, Gaisford S et al (2015b) 3D printing of medicines: engineering novel oral devices with unique design and drug release characteristics. Mol Pharm 12(11):4077–4084. doi:10.1021/acs.molpharmaceut.5b00510

Grohganz H, Löbmann K, Priemel P, Tarp Jensen K, Graeser K, Strachan C et al (2013) Amorphous drugs and dosage forms. J Drug Deliv Sci Technol 23(4):403–408. doi:10.1016/S1773-2247(13)50057-8

Gross BC, Erkal JL, Lockwood SY, Chen C, Spence DM (2014) Evaluation of 3D printing and its potential impact on biotechnology and the chemical sciences. Anal Chem 86(7):3240–3253. doi:10.1021/ac403397r

Günther D, Heymel B, Franz Günther J, Ederer I (2014) Continuous 3D-printing for additive manufacturing. Rapid Prototyping J 20(4):320–327. doi:10.1108/RPJ-08-2012-0068

Gynther M, Laine K, Ropponen J, Leppänen J, Mannila A, Nevalainen T et al (2008) Large neutral amino acid transporter enables brain drug delivery via prodrugs. J Med Chem 51(4):932–936. doi:10.1021/jm701175d

Hamid Q, Snyder J, Wang C, Timmer M, Hammer J, Guceri S et al (2011) Fabrication of three-dimensional scaffolds using precision extrusion deposition with an assisted cooling device. Biofabrication 3(3):034109

Hancock BC (2002) Disordered drug delivery: destiny, dynamics and the Deborah number. J Pharm Pharmacol 54(6):737–746

Hancock BC, Zografi G (1997) Characteristics and significance of the amorphous state in pharmaceutical systems. J Pharm Sci 86(1):1–12. doi:10.1021/js9601896

Hancock BC, Shamblin SL, Zografi G (1995) Molecular mobility of amorphous pharmaceutical solids below their glass transition temperatures. Pharm Res 12(6):799–806

Heikkilä T, Santos HA, Kumar N, Murzin DY, Salonen J, Laaksonen T et al (2010) Cytotoxicity study of ordered mesoporous silica MCM-41 and SBA-15 microparticles on Caco-2 cells. Eur J Pharm Biopharm 74(3):483–494. doi:10.1016/j.ejpb.2009.12.006

Hirano A, Kameda T, Arakawa T, Shiraki K (2010) Arginine-assisted solubilization system for drug substances: solubility experiment and simulation. J Phys Chem B 114(42):13455–13462. doi:10.1021/jp101909a

Hoque ME, Chuan YL, Pashby I (2012) Extrusion based rapid prototyping technique: an advanced platform for tissue engineering scaffold fabrication. Biopolymers 97(2):83–93. doi:10.1002/bip.21701

Hu Y, Wang J, Zhi Z, Jiang T, Wang S (2011) Facile synthesis of 3D cubic mesoporous silica microspheres with a controllable pore size and their application for improved delivery of a water-insoluble drug. J Colloid Interface Sci 363(1):410–417. doi:10.1016/j.jcis.2011.07.022

Hughey J, DiNunzio J, Bennett R, Brough C, Miller D, Ma H et al (2010) Dissolution enhancement of a drug exhibiting thermal and acidic decomposition characteristics by fusion processing: a comparative study of hot melt extrusion and KinetiSol® dispersing. AAPS PharmSciTech 11(2):760–774. doi:10.1208/s12249-010-9431-y

Hughey JR, Keen JM, Brough C, Saeger S, McGinity JW (2011) Thermal processing of a poorly water-soluble drug substance exhibiting a high melting point: the utility of KinetiSol® dispersing. Int J Pharm 419(1–2):222–230. doi:10.1016/j.ijpharm.2011.08.007

Hughey JR, Keen JM, Miller DA, Brough C, McGinity JW (2012) Preparation and characterization of fusion processed solid dispersions containing a viscous thermally labile polymeric carrier. Int J Pharm 438(1–2):11–19. doi:10.1016/j.ijpharm.2012.08.032

Hughey JR, Keen JM, Miller DA, Kolter K, Langley N, McGinity JW (2013) The use of inorganic salts to improve the dissolution characteristics of tablets containing Soluplus®-based solid dispersions. Eur J Pharm Sci 48(4–5):758–766. doi:10.1016/j.ejps.2013.01.004

Hughey JR, Keen JM, Bennett RC, Obara S, McGinity JW (2014) The incorporation of low-substituted hydroxypropyl cellulose into solid dispersion systems. Drug Dev Ind Pharm 41:1294–1301

Igantious F, Sun L, Inventors (2004) Electrospun amorphous pharmaceutical compositions patent WO2004014304

Ignatious F, Sun L, Lee C-P, Baldoni J (2010) Electrospun nanofibers in oral drug delivery. Pharm Res 27(4):576–588

Inagaki S, Fukushima Y, Kuroda K (1993) Synthesis of highly ordered mesoporous materials from a layered polysilicate. J Chem Soc Chem Commun 8:680–682. doi:10.1039/C39930000680

Iulia D, Ursan BLC, Andrea Pierce BS (2003) Three-dimensional drug printing: a structured review. J Am Pharm Assoc 53:136–144. doi:10.1331/JAPhA.2013.12217

Janssens S, Van den Mooter G (2009) Review: physical chemistry of solid dispersions. J Pharm Pharmacol 61(12):1571–1586. doi:10.1211/jpp.61.12.0001

Jensen KT, Blaabjerg LI, Lenz E, Bohr A, Grohganz H, Kleinebudde P et al (2015a) Preparation and characterization of spray-dried co-amorphous drug–amino acid salts. J Pharm Pharmacol 68(5):615–624. doi:10.1111/jphp.12458

Jensen KT, Larsen FH, Cornett C, Löbmann K, Grohganz H, Rades T (2015b) Formation mechanism of coamorphous drug–amino acid mixtures. Mol Pharm 12(7):2484–2492. doi:10.1021/acs.molpharmaceut.5b00295

Jiang H, Wang T, Wang L, Sun C, Jiang T, Cheng G et al (2012) Development of an amorphous mesoporous TiO_2 nanosphere as a novel carrier for poorly water-soluble drugs: effect of different crystal forms of TiO_2 carriers on drug loading and release behaviors. Micropor Mesopor Mater 153:124–130. doi:10.1016/j.micromeso.2011.12.013

Keen JM, Hughey JR, Bennett RC, Jannin V, Rosiaux Y, Marchaud D et al (2015) Effect of tablet structure on controlled release from supersaturating solid dispersions containing glyceryl behenate. Mol Pharm 12(1):120–126. doi:10.1021/mp500480y

Kenawy E-R, Bowlin GL, Mansfield K, Layman J, Simpson DG, Sanders EH et al (2002) Release of tetracycline hydrochloride from electrospun poly (ethylene-co-vinylacetate), poly (lactic acid), and a blend. J Control Release 81(1):57–64

Kim M-S (2013) Soluplus-coated colloidal silica nanomatrix system for enhanced supersaturation and oral absorption of poorly water-soluble drugs. Artif Cells Nanomed Biotechnol 41(6):363–367

Kim T-W, Chung P-W, Slowing II, Tsunoda M, Yeung ES, Lin VSY (2008) Structurally ordered mesoporous carbon nanoparticles as transmembrane delivery vehicle in human cancer cells. Nano Lett 8(11):3724–3727. doi:10.1021/nl801976m

Kinnari P, Mäkilä E, Heikkilä T, Salonen J, Hirvonen J, Santos HA (2011) Comparison of mesoporous silicon and non-ordered mesoporous silica materials as drug carriers for itraconazole. Int J Pharm 414(1–2):148–156. doi:10.1016/j.ijpharm.2011.05.021

Knapik J, Wojnarowska Z, Grzybowska K, Jurkiewicz K, Tajber L, Paluch M (2015) Molecular dynamics and physical stability of coamorphous ezetimib and indapamide mixtures. Mol Pharm 12(10):3610–3619. doi:10.1021/acs.molpharmaceut.5b00334

Kresge C, Leonowicz M, Roth W, Vartuli J, Beck J (1992) Ordered mesoporous molecular sieves synthesized by a liquid-crystal template mechanism. Nature 359(6397):710–712

Kruk M, Jaroniec M, Ko CH, Ryoo R (2000) Characterization of the porous structure of SBA-15. Chem Mater 12(7):1961–1968

Kulig K, David B-O, Cantrill SV, Rosen P, Rumack BH (1985) Management of acutely poisoned patients without gastric emptying. Ann Emerg Med 14(6):562–567. doi:10.1016/S0196-0644(85)80780-0

Kumar A, Ganjyal GM, Jones DD, Hanna MA (2008) Modeling residence time distribution in a twin-screw extruder as a series of ideal steady-state flow reactors. J Food Eng 84(3):441–448

LaFountaine J, Prasad L, Brough C, Miller D, McGinity J, Williams R III (2015a) Thermal processing of PVP- and HPMC-based amorphous solid dispersions. AAPS PharmSciTech 17(1):120–132. doi:10.1208/s12249-015-0417-7

LaFountaine JS, McGinity JW, Williams RO III (2015b) Challenges and strategies in thermal processing of amorphous solid dispersions: a review. AAPS PharmSciTech 17(1):43–55

Laitinen R, Löbmann K, Strachan CJ, Grohganz H, Rades T (2013) Emerging trends in the stabilization of amorphous drugs. Int J Pharm 453(1):65–79. doi:10.1016/j.ijpharm.2012.04.066

Laitinen R, Löbmann K, Grohganz H, Strachan C, Rades T (2014) Amino acids as co-amorphous excipients for simvastatin and glibenclamide: physical properties and stability. Mol Pharm 11(7):2381–2389. doi:10.1021/mp500107s

Lakshman JP, Cao Y, Kowalski J, Serajuddin ATM (2008) Application of melt extrusion in the development of a physically and chemically stable high-energy amorphous solid dispersion of a poorly water-soluble drug. Mol Pharm 5(6):994–1002. doi:10.1021/mp8001073

Lenz E, Jensen KT, Blaabjerg LI, Knop K, Grohganz H, Löbmann K et al (2015) Solid-state properties and dissolution behaviour of tablets containing co-amorphous indomethacin–arginine. Eur J Pharm Biopharm 96:44–52. doi:10.1016/j.ejpb.2015.07.011

Leuner C, Dressman J (2000) Improving drug solubility for oral delivery using solid dispersions. Eur J Pharm Biopharm 50(1):47–60. doi:10.1016/S0939-6411(00)00076-X

Liang C, Li Z, Dai S (2008) Mesoporous carbon materials: synthesis and modification. Angew Chem Int Ed 47(20):3696–3717. doi:10.1002/anie.200702046

Lipinski CA (2004) Lead-and drug-like compounds: the rule-of-five revolution. Drug Discov Today Technol 1(4):337–341

Lipinski CA, Lombardo F, Dominy BW, Feeney PJ (2001) Experimental and computational approaches to estimate solubility and permeability in drug discovery and development settings. Adv Drug Deliv Rev 46(1–3):3–26. doi:10.1016/S0169-409X(00)00129-0

Liu K-S, Liu H, Qi J-H, Liu Q-Y, Liu Z, Xia M et al (2012) SNX-2112, an Hsp90 inhibitor, induces apoptosis and autophagy via degradation of Hsp90 client proteins in human melanoma A-375 cells. Cancer Lett 318(2):180–188

Löbmann K, Laitinen R, Grohganz H, Gordon KC, Strachan C, Rades T (2011) Coamorphous drug systems: enhanced physical stability and dissolution rate of indomethacin and naproxen. Mol Pharm 8(5):1919–1928. doi:10.1021/mp2002973

Löbmann K, Strachan C, Grohganz H, Rades T, Korhonen O, Laitinen R (2012) Co-amorphous simvastatin and glipizide combinations show improved physical stability without evidence of intermolecular interactions. Eur J Pharm Biopharm 81(1):159–169. doi:10.1016/j.ejpb.2012.02.004

Löbmann K, Grohganz H, Laitinen R, Strachan C, Rades T (2013a) Amino acids as co-amorphous stabilizers for poorly water soluble drugs—part 1: preparation, stability and dissolution enhancement. Eur J Pharm Biopharm 85(3, Part B):873–881. doi:10.1016/j.ejpb.2013.03.014

Löbmann K, Laitinen R, Grohganz H, Strachan C, Rades T, Gordon KC (2013b) A theoretical and spectroscopic study of co-amorphous naproxen and indomethacin. Int J Pharm 453(1):80–87. doi:10.1016/j.ijpharm.2012.05.016

Löbmann K, Laitinen R, Strachan C, Rades T, Grohganz H (2013c) Amino acids as co-amorphous stabilizers for poorly water-soluble drugs—part 2: molecular interactions. Eur J Pharm Biopharm 85(3):882–888. doi:10.1016/j.ejpb.2013.03.026

Löbmann K, Jensen KT, Laitinen R, Rades T, Strachan CJ, Grohganz H (2014) Stabilized amorphous solid dispersions with small molecule excipients. In: Shah N, Sandhu H, Choi DS, Chokshi H, Malick AW (eds) Amorphous solid dispersions. Advances in delivery science and technology. Springer, New York, pp 613–636

Lu Q, Zografi G (1998) Phase behavior of binary and ternary amorphous mixtures containing indomethacin, citric acid, and PVP. Pharm Res 15(8):1202–1206. doi:10.1023/A:1011983606606

Lu J, Liong M, Sherman S, Xia T, Kovochich M, Nel A et al (2007) Mesoporous silica nanoparticles for cancer therapy: energy-dependent cellular uptake and delivery of paclitaxel to cancer cells. Nanobiotechnol 3(2):89–95. doi:10.1007/s12030-008-9003-3

Ma T-Y, Liu L, Yuan Z-Y (2013) Direct synthesis of ordered mesoporous carbons. Chem Soc Rev 42(9):3977–4003. doi:10.1039/C2CS35301F

Maeng H-J, Kim E-S, Chough C, Joung M, Lim JW, Shim C-K et al (2014) Addition of amino acid moieties to lapatinib increases the anti-cancer effect via amino acid transporters. Biopharm Drug Dispos 35(1):60–69. doi:10.1002/bdd.1872

Malone E, Lipson H (2007) Fab@ Home: the personal desktop fabricator kit. Rapid Prototyping J 13(4):245–255

Mamaeva V, Sahlgren C, Lindén M (2013) Mesoporous silica nanoparticles in medicine—recent advances. Adv Drug Deliv Rev 65(5):689–702

Masuda T, Yoshihashi Y, Yonemochi E, Fujii K, Uekusa H, Terada K (2012) Cocrystallization and amorphization induced by drug–excipient interaction improves the physical properties of acyclovir. Int J Pharm 422(1):160–169

Mekaru H, Lu J, Tamanoi F (2015) Development of mesoporous silica-based nanoparticles with controlled release capability for cancer therapy. Adv Drug Deliv Rev 95:40–49. doi:10.1016/j.addr.2015.09.009

Mellaerts R, Jammaer JAG, Van Speybroeck M, Chen H, Humbeeck JV, Augustijns P et al (2008a) Physical state of poorly water soluble therapeutic molecules loaded into SBA-15 ordered mesoporous silica carriers: a case study with itraconazole and ibuprofen. Langmuir 24(16):8651–8659. doi:10.1021/la801161g

Mellaerts R, Mols R, Jammaer JAG, Aerts CA, Annaert P, Van Humbeeck J et al (2008b) Increasing the oral bioavailability of the poorly water soluble drug itraconazole with ordered mesoporous silica. Eur J Pharm Biopharm 69(1):223–230. doi:10.1016/j.ejpb.2007.11.006

Mellaerts R, Houthoofd K, Elen K, Chen H, Van Speybroeck M, Van Humbeeck J et al (2010) Aging behavior of pharmaceutical formulations of itraconazole on SBA-15 ordered mesoporous silica carrier material. Micropor Mesopor Mater 130(1–3):154–161. doi:10.1016/j.micromeso.2009.10.026

Meng H, Liong M, Xia T, Li Z, Ji Z, Zink JI et al (2010) Engineered design of mesoporous silica nanoparticles to deliver doxorubicin and P-glycoprotein siRNA to overcome drug resistance in a cancer cell line. ACS Nano 4(8):4539–4550. doi:10.1021/nn100690m

Miller DA (2007) Improved oral absorption of poorly water-soluble drugs by advanced solid dispersion systems. PhD dissertation. The University of Texas at Austin, Austin, TX

Mizushima Y, Ikoma T, Tanaka J, Hoshi K, Ishihara T, Ogawa Y et al (2006) Injectable porous hydroxyapatite microparticles as a new carrier for protein and lipophilic drugs. J Control Release 110(2):260–265. doi:10.1016/j.jconrel.2005.09.051

Muñoz B, Rámila A, Pérez-Pariente J, Díaz I, Vallet-Regí M (2003) MCM-41 organic modification as drug delivery rate regulator. Chem Mater 15(2):500–503. doi:10.1021/cm021217q

Mura P, Maestrelli F, Cirri M (2003) Ternary systems of naproxen with hydroxypropyl-β-cyclodextrin and aminoacids. Int J Pharm 260(2):293–302. doi:10.1016/S0378-5173(03)00265-5

Mura P, Bettinetti GP, Cirri M, Maestrelli F, Sorrenti M, Catenacci L (2005) Solid-state characterization and dissolution properties of Naproxen–Arginine–Hydroxypropyl-β-cyclodextrin ternary system. Eur J Pharm Biopharm 59(1):99–106. doi:10.1016/j.ejpb.2004.05.005

Murphy DK, Rabel S (2008) Thermal analysis and calorimetric methods for the characterization of new crystal forms. Drugs Pharm Sci 178:279

Nagy ZK, Balogh A, Vajna B, Farkas A, Patyi G, Kramarics Á et al (2012) Comparison of electrospun and extruded soluplus®-based solid dosage forms of improved dissolution. J Pharm Sci 101(1):322–332. doi:10.1002/jps.22731

Nagy ZK, Balogh A, Drávavölgyi G, Ferguson J, Pataki H, Vajna B et al (2013) Solvent-free melt electrospinning for preparation of fast dissolving drug delivery system and comparison with solvent-based electrospun and melt extruded systems. J Pharm Sci 102(2):508–517. doi:10.1002/jps.23374

Nakamatsu J, Torres FG, Troncoso OP, Min-Lin Y, Boccaccini AR (2006) Processing and characterization of porous structures from chitosan and starch for tissue engineering scaffolds. Biomacromolecules 7(12):3345–3355. doi:10.1021/bm0605311

Neuvonen P, Olkkola K (1988) Oral activated charcoal in the treatment of intoxications. Med Toxicol Adverse Drug Exp 3(1):33–58. doi:10.1007/BF03259930

Oh WK, Yoon H, Jang J (2010) Size control of magnetic carbon nanoparticles for drug delivery. Biomaterials 31(6):1342–1348. doi:10.1016/j.biomaterials.2009.10.018

Peng H, Dong R, Wang S, Zhang Z, Luo M, Bai C et al (2013) A pH-responsive nano-carrier with mesoporous silica nanoparticles cores and poly(acrylic acid) shell-layers: fabrication, characterization and properties for controlled release of salidroside. Int J Pharm 446(1–2):153–159. doi:10.1016/j.ijpharm.2013.01.071

Qu F, Zhu G, Huang S, Li S, Qiu S (2006) Effective controlled release of captopril by silylation of mesoporous MCM-41. ChemPhysChem 7(2):400–406

Reneker DH, Chun I (1996) Nanometre diameter fibres of polymer, produced by electrospinning. Nanotechnology 7(3):216

Repka MA, Gerding TG, Repka SL, McGinity JW (1999) Influence of plasticizers and drugs on the physical-mechanical properties of hydroxypropylcellulose films prepared by hot melt extrusion. Drug Dev Ind Pharm 25(5):625–633

Repka MA, Prodduturi S, Stodghill SP (2003) Production and characterization of hot-melt extruded films containing clotrimazole. Drug Dev Ind Pharm 29(7):757–765

Roberts AD, Zhang H (2013) Poorly water-soluble drug nanoparticles via solvent evaporation in water-soluble porous polymers. Int J Pharm 447(1–2):241–250. doi:10.1016/j.ijpharm.2013.03.001

Rosenholm JM, Sahlgren C, Linden M (2010) Towards multifunctional, targeted drug delivery systems using mesoporous silica nanoparticles—opportunities & challenges. Nanoscale 2(10):1870–1883. doi:10.1039/C0NR00156B

Rowe CW, Katstra WE, Palazzolo RD, Giritlioglu B, Teung P, Cima MJ (2000) Multimechanism oral dosage forms fabricated by three dimensional printing™. J Control Release 66(1):11–17. doi:10.1016/S0168-3659(99)00224-2

Rowe RC, Sheskey PJ, Cook WG, Fenton ME, American Pharmacists A (2012) Handbook of pharmaceutical excipients. Pharmaceutical Press, London

Saha D, Warren KE, Naskar AK (2014a) Controlled release of antipyrine from mesoporous carbons. Micropor Mesopor Mater 196:327–334. doi:10.1016/j.micromeso.2014.05.024

Saha D, Warren KE, Naskar AK (2014b) Soft-templated mesoporous carbons as potential materials for oral drug delivery. Carbon 71:47–57. doi:10.1016/j.carbon.2014.01.005

Saha D, Moken T, Chen J, Hensley DK, Delaney K, Hunt MA et al (2015) Micro-/mesoporous carbons for controlled release of antipyrine and indomethacin. RSC Adv 5(30):23699–23707. doi:10.1039/C5RA00251F

Sandler N, Salmela I, Fallarero A, Rosling A, Khajeheian M, Kolakovic R et al (2014) Towards fabrication of 3D printed medical devices to prevent biofilm formation. Int J Pharm 459(1–2):62–64. doi:10.1016/j.ijpharm.2013.11.001

Sekiguchi K, Obi N (1961) Studies on absorption of eutectic mixture. I. A comparison of the behavior of eutectic mixture of sulfathiazole and that of ordinary sulfathiazole in man. Chem Pharm Bull 9(11):866–872

Serajuddin A (1999) Solid dispersion of poorly water-soluble drugs: early promises, subsequent problems, and recent breakthroughs. J Pharm Sci 88(10):1058–1066

Shen SC, Ng WK, Chia L, Dong YC, Tan RB (2010) Stabilized amorphous state of ibuprofen by co-spray drying with mesoporous SBA-15 to enhance dissolution properties. J Pharm Sci 99(4):1997–2007

Skowyra J, Pietrzak K, Alhnan MA (2015) Fabrication of extended-release patient-tailored prednisolone tablets via fused deposition modelling (FDM) 3D printing. Eur J Pharm Sci 68:11–17. doi:10.1016/j.ejps.2014.11.009

Slowing I, Trewyn BG, Lin VSY (2006) Effect of surface functionalization of MCM-41-type mesoporous silica nanoparticles on the endocytosis by human cancer cells. J Am Chem Soc 128(46):14792–14793. doi:10.1021/ja0645943

Song S-W, Hidajat K, Kawi S (2005) Functionalized SBA-15 materials as carriers for controlled drug delivery: influence of surface properties on matrix-drug interactions. Langmuir 21(21):9568–9575

Tang Q, Xu Y, Wu D, Sun Y (2006) A study of carboxylic-modified mesoporous silica in controlled delivery for drug famotidine. J Solid State Chem 179(5):1513–1520

Tang Q, Chen Y, Chen J, Li J, Xu Y, Wu D et al (2010) Drug delivery from hydrophobic-modified mesoporous silicas: control via modification level and site-selective modification. J Solid State Chem 183(1):76–83

Teja A, Musmade PB, Khade AB, Dengale SJ (2015) Simultaneous improvement of solubility and permeability by fabricating binary glassy materials of Talinolol with Naringin: solid state characterization, in-vivo in-situ evaluation. Eur J Pharm Sci 78:234–244. doi:10.1016/j.ejps.2015.08.002

Thomas MJK, Slipper I, Walunj A, Jain A, Favretto ME, Kallinteri P et al (2010) Inclusion of poorly soluble drugs in highly ordered mesoporous silica nanoparticles. Int J Pharm 387(1–2):272–277. doi:10.1016/j.ijpharm.2009.12.023

Trasi NS, Taylor LS (2015) Dissolution performance of binary amorphous drug combinations—impact of a second drug on the maximum achievable supersaturation. Int J Pharm 496(2):282–290. doi:10.1016/j.ijpharm.2015.10.026

Tsume Y, Hilfinger J, Amidon G (2011) Potential of amino acid/dipeptide monoester prodrugs of floxuridine in facilitating enhanced delivery of active drug to interior sites of tumors: a two-tier monolayer in vitro study. Pharm Res 28(10):2575–2588. doi:10.1007/s11095-011-0485-7

Ukmar T, Planinšek O (2010) Ordered mesoporous silicates as matrices for controlled release of drugs. Acta Pharm 60(4):373–385

Vallet-Regi M, Rámila A, del Real RP, Pérez-Pariente J (2001) A new property of MCM-41: drug delivery system. Chem Mater 13(2):308–311. doi:10.1021/cm0011559

Van Speybroeck M, Mols R, Mellaerts R, Thi TD, Martens JA, Humbeeck JV et al (2010) Combined use of ordered mesoporous silica and precipitation inhibitors for improved oral absorption of the poorly soluble weak base itraconazole. Eur J Pharm Biopharm 75(3):354–365. doi:10.1016/j.ejpb.2010.04.009

Verreck G (2012) The influence of plasticizers in hot-melt extrusion. Hot-Melt Extrusion: Pharmaceutical Applications:93–112

Verreck G, Chun I, Peeters J, Rosenblatt J, Brewster ME (2003a) Preparation and characterization of nanofibers containing amorphous drug dispersions generated by electrostatic spinning. Pharm Res 20(5):810–817

Verreck G, Chun I, Rosenblatt J, Peeters J, Van Dijck A, Mensch J et al (2003b) Incorporation of drugs in an amorphous state into electrospun nanofibers composed of a water-insoluble, nonbiodegradable polymer. J Control Release 92(3):349–360

Verreck G, Decorte A, Heymans K, Adriaensen J, Liu D, Tomasko D et al (2006) Hot stage extrusion of p-amino salicylic acid with EC using CO 2 as a temporary plasticizer. Int J Pharm 327(1):45–50

Vialpando M, Aerts A, Persoons J, Martens J, Van Den Mooter G (2011) Evaluation of ordered mesoporous silica as a carrier for poorly soluble drugs: influence of pressure on the structure and drug release. J Pharm Sci 100(8):3411–3420. doi:10.1002/jps.22535

Vialpando M, Backhuijs F, Martens JA, Van den Mooter G (2012) Risk assessment of premature drug release during wet granulation of ordered mesoporous silica loaded with poorly soluble compounds itraconazole, fenofibrate, naproxen, and ibuprofen. Eur J Pharm Biopharm 81(1):190–198. doi:10.1016/j.ejpb.2012.01.012

Wang F, Shor L, Darling A, Khalil S, Sun W, Güçeri S et al (2004) Precision extruding deposition and characterization of cellular poly-ε-caprolactone tissue scaffolds. Rapid Prototyping J 10(1):42–49. doi:10.1108/13552540410512525

Wang G, Otuonye AN, Blair EA, Denton K, Tao Z, Asefa T (2009) Functionalized mesoporous materials for adsorption and release of different drug molecules: a comparative study. J Solid State Chem 182(7):1649–1660

Wang F, Hui H, Barnes TJ, Barnett C, Prestidge CA (2010) Oxidized mesoporous silicon microparticles for improved oral delivery of poorly soluble drugs. Mol Pharm 7(1):227–236. doi:10.1021/mp900221e

Wang X, Liu P, Tian Y (2011a) Ordered mesoporous carbons for ibuprofen drug loading and release behavior. Micropor Mesopor Mater 142(1):334–340. doi:10.1016/j.micromeso.2010.12.018

Wang X, Liu P, Tian Y, Zang L (2011b) Novel synthesis of Fe-containing mesoporous carbons and their release of ibuprofen. Micropor Mesopor Mater 145(1–3):98–103. doi:10.1016/j.micromeso.2011.04.033

Wang Y, Zhao Q, Hu Y, Sun L, Bai L, Jiang T et al (2013) Ordered nanoporous silica as carriers for improved delivery of water insoluble drugs: a comparative study between three dimensional and two dimensional macroporous silica. Int J Nanomedicine 8:4015–4031. doi:10.2147/IJN.S52605

Wang T, Zhao P, Zhao Q, Wang B, Wang S (2014) The mechanism for increasing the oral bioavailability of poorly water-soluble drugs using uniform mesoporous carbon spheres as a carrier. Drug Deliv 23:420–428

Wang Y, Zhao Q, Han N, Bai L, Li J, Liu J et al (2015) Mesoporous silica nanoparticles in drug delivery and biomedical applications. Nanomed Nanotechnol Biol Med 11(2):313–327. doi:10.1016/j.nano.2014.09.014

Wu C, Wang Z, Zhi Z, Jiang T, Zhang J, Wang S (2011) Development of biodegradable porous starch foam for improving oral delivery of poorly water soluble drugs. Int J Pharm 403(1–2):162–169. doi:10.1016/j.ijpharm.2010.09.040

Xu W, Gao Q, Xu Y, Wu D, Sun Y, Shen W et al (2008) Controlled drug release from bifunctionalized mesoporous silica. J Solid State Chem 181(10):2837–2844

Xu W, Riikonen J, Lehto V-P (2013) Mesoporous systems for poorly soluble drugs. Int J Pharm 453(1):181–197. doi:10.1016/j.ijpharm.2012.09.008

Yachamaneni S, Yushin G, Yeon S-H, Gogotsi Y, Howell C, Sandeman S et al (2010) Mesoporous carbide-derived carbon for cytokine removal from blood plasma. Biomaterials 31(18):4789–4794

Yamamura S, Momose Y, Takahashi K, Nagatani S (1996) Solid-state interaction between cimetidine and naproxen. Drug Stability 1:173–178

Yamamura S, Gotoh H, Sakamoto Y, Momose Y (2000) Physicochemical properties of amorphous precipitates of cimetidine–indomethacin binary system. Eur J Pharm Biopharm 49(3):259–265. doi:10.1016/S0939-6411(00)00060-6

Yamamura S, Gotoh H, Sakamoto Y, Momose Y (2002) Physicochemical properties of amorphous salt of cimetidine and diflunisal system. Int J Pharm 241(2):213–221. doi:10.1016/S0378-5173(02)00195-3

Yang Q, Wang S, Fan P, Wang L, Di Y, Lin K et al (2005) pH-responsive carrier system based on carboxylic acid modified mesoporous silica and polyelectrolyte for drug delivery. Chem Mater 17(24):5999–6003

Yang P, Gai S, Lin J (2012) Functionalized mesoporous silica materials for controlled drug delivery. Chem Soc Rev 41(9):3679–3698. doi:10.1039/C2CS15308D

Ye F, Guo H, Zhang H, He X (2010) Polymeric micelle-templated synthesis of hydroxyapatite hollow nanoparticles for a drug delivery system. Acta Biomater 6(6):2212–2218

Yu D-G, Zhu L-M, Branford-White CJ, Yang J-H, Wang X, Li Y et al (2011) Solid dispersions in the form of electrospun core-sheath nanofibers. Int J Nanomedicine 6:3271–3280. doi:10.2147/IJN.S27468

Zhang C, Li C, Huang S, Hou Z, Cheng Z, Yang P et al (2010a) Self-activated luminescent and mesoporous strontium hydroxyapatite nanorods for drug delivery. Biomaterials 31(12):3374–3383

Zhang Y, Zhi Z, Jiang T, Zhang J, Wang Z, Wang S (2010b) Spherical mesoporous silica nanoparticles for loading and release of the poorly water-soluble drug telmisartan. J Control Release 145(3):257–263. doi:10.1016/j.jconrel.2010.04.029

Zhang Y, Zhang J, Jiang T, Wang S (2011) Inclusion of the poorly water-soluble drug simvastatin in mesocellular foam nanoparticles: drug loading and release properties. Int J Pharm 410(1–2):118–124. doi:10.1016/j.ijpharm.2010.07.040

Zhang Y, Wang J, Bai X, Jiang T, Zhang Q, Wang S (2012) Mesoporous Silica Nanoparticles for Increasing the Oral Bioavailability and Permeation of Poorly Water Soluble Drugs. Mol Pharm 9(3):505–513. doi:10.1021/mp200287c

Zhang Y, Zhi Z, Li X, Gao J, Song Y (2013) Carboxylated mesoporous carbon microparticles as new approach to improve the oral bioavailability of poorly water-soluble carvedilol. Int J Pharm 454(1):403–411. doi:10.1016/j.ijpharm.2013.07.009

Zhang L, Li Y, Jin Z, Chan KM, Yu JC (2015a) Mesoporous carbon/CuS nanocomposites for pH-dependent drug delivery and near-infrared chemo-photothermal therapy. RSC Adv 5(113):93226–93233. doi:10.1039/C5RA19458J

Zhang X, Zhang T, Ye Y, Chen H, Sun H, Zhou X et al (2015b) Phospholipid-stabilized mesoporous carbon nanospheres as versatile carriers for systemic delivery of amphiphobic SNX-2112 (a Hsp90 inhibitor) with enhanced antitumor effect. Eur J Pharm Biopharm 94:30–41. doi:10.1016/j.ejpb.2015.04.023

Zhang Y, Zhao Q, Zhu W, Zhang L, Han J, Lin Q et al (2015c) Synthesis and evaluation of mesoporous carbon/lipid bilayer nanocomposites for improved oral delivery of the poorly water-soluble drug, nimodipine. Pharm Res 32(7):2372–2383. doi:10.1007/s11095-015-1630-5

Zhao D, Feng J, Huo Q, Melosh N, Fredrickson GH, Chmelka BF et al (1998) Triblock copolymer syntheses of mesoporous silica with periodic 50 to 300 angstrom pores. Science 279(5350):548–552

Zhao P, Jiang H, Jiang T, Zhi Z, Wu C, Sun C et al (2012a) Inclusion of celecoxib into fibrous ordered mesoporous carbon for enhanced oral bioavailability and reduced gastric irritancy. Eur J Pharm Sci 45(5):639–647. doi:10.1016/j.ejps.2012.01.003

Zhao P, Wang L, Sun C, Jiang T, Zhang J, Zhang Q et al (2012b) Uniform mesoporous carbon as a carrier for poorly water soluble drug and its cytotoxicity study. Eur J Pharm Biopharm 80(3):535–543. doi:10.1016/j.ejpb.2011.12.002

Zhao Q, Wang T, Wang J, Zheng L, Jiang T, Cheng G et al (2012c) Fabrication of mesoporous hydroxycarbonate apatite for oral delivery of poorly water-soluble drug carvedilol. J Non-Crystal Solids 358(2):229–235. doi:10.1016/j.jnoncrysol.2011.09.020

Zhu Y, Shah NH, Malick AW, Infeld MH, McGinity JW (2002) Solid-state plasticization of an acrylic polymer with chlorpheniramine maleate and triethyl citrate. Int J Pharm 241(2):301–310

Zhu Y, Mehta KA, McGinity JW (2006) Influence of plasticizer level on the drug release from sustained release film coated and hot-melt extruded dosage forms. Pharm Dev Technol 11(3):285–294

Zhu S, Chen C, Chen Z, Liu X, Li Y, Shi Y et al (2011) Thermo-responsive polymer-functionalized mesoporous carbon for controlled drug release. Mater Chem Phys 126(1–2):357–363. doi:10.1016/j.matchemphys.2010.11.013

Zhu J, Liao L, Bian X, Kong J, Yang P, Liu B (2012) pH-controlled delivery of doxorubicin to cancer cells, based on small mesoporous carbon nanospheres. Small 8(17):2715–2720